Extraction and characterization of hardness causing minerals present in tap water to study its adsorption and catalysis

A thesis

Submitted in the partial fulfillment of the requirements for the award of degree of

MASTER OF SCIENCE

in

CHEMISTRY

Submitted by

Deepak Singla
(Roll No. 301602013)

Under the supervision of

Dr. Bonamali Pal
Professor

School of Chemistry and Biochemistry
Thapar Institute of Engineering & Technology
Patiala-147004

June, 2018

Certificate

I hereby certify that the work presented in this thesis entitled "**Extraction and Characterization of hardness causing minerals present in tap water to study its adsorption and catalysis**" submitted in partial fulfillment of the requirements for the award of degree of Master of Science in Chemistry submitted to School of Chemistry and Biochemistry, Thapar Institute of Engineering and Technology, Patiala is an authentic record of my own work carried out under the supervision of Dr. Bonamali Pal. The matter of my thesis has not been submitted to any other University for the award of any other degree or diploma.

Date: 31.07.2018

Deepak Singla

Deepak Singla

This is to certify that the above statement made by the candidate is correct and true to the best of our knowledge.

Dr. Bonamali Pal
Professor
School of Chemistry and Biochemistry
Thapar Institute of Engineering and Technology, Patiala- 147004

Acknowledgment

I am thankful to my supervisor Dr. Bonamali Pal, Professor, SCBC, Thapar Institute of Engineering and Technology for his innovative ideas, presence, and valuable words and also scolded so that I may learn something. He discussed about my work daily and gave appropriate suggestions for it.

I am deeply thankful to Dr. Amjad Ali, Associate Professor and Head, School Of Chemistry and Bio-Chemistry for giving me this opportunity to work and allowed me to use various facilities in the department.

I would like to thank my lab research scholars Mr. Aadil Bathla, Miss. Tanushree Basu, and Miss Manpreet Kaur for sharing their experience and helped a lot in my lab work. I am also thankful to Chandra Sir and Hemant for their help.

I am also thankful to my friends Mitresh Malhotra, Kartik Sharma, Anurag Yadav, Ajit Seth and Shantanu Aggarwal for always motivating me and helping me whenever I needed.

Above all I am thankful to my parents for their blessings, support and encouragement.

Date: **Deepak Singla**

Abstract

The present work describes the extraction and characterization of hardness causing minerals obtained from tap water boiling (TWB). The extracted residues were centrifuged (8000 rpm, 5 min, 25ºC) and washed three times with water, ethanol, respectively. Later on, it was dried at room temperature. The powder form of this residue (RMP-TWB) was further sintered at 400ºC and 900ºC for 4 h in the furnace. It was characterized by using DLS, XRD, SEM, FTIR, BET and UV- Visible spectroscopy techniques etc. Then this powder was used to investigate its adsorption and photocatalytic properties for removal and degradation of Malachite Green (MG) dye under a sunlight irradiation. DLS measurements showed that the particle size distribution of RMP-TWB lies in the range between from 0.163 µm to 726 µm. XRD data revealed that RMP-TWB contains the majority of the calcium carbonate ($CaCO_3$) and some amount of MgO, SiO_2 etc. The surface morphology of residue showed the sphere, rod-like shapes and the particle size lies between 1µm to 10µm. From BET and BJH analysis, the surface area and mean pore diameter of RMP-TWB was found to be $35.4 m^2 g^{-1}$ and 10.08 nm, respectively. The impact of different parameters likes concentration of MG dye; the amount of adsorbent on adsorption was also studied. The adsorption curve follows the Freundlich adsorption isotherm. The degradation of MG dye under sunlight irradiation was studied at different intervals of time and measured its kinetics studies by zero and first order reaction. The results showed that after 60 to 90 min sunlight irradiation maximum degradation of MG dye was observed. It was concluded that this hardness causing minerals will be very effective for adsorption, removal, and degradation of toxic industrial MG dye in the presence of sunlight.

List of abbreviations

RT: Room temperature

MG: Malachite green.

TWB: boiling/distillation of tap water.

RML-TWB: Liquid form of residues metal salt and carbonate material from boiling/distillation tap water.

RMP-TWB: Powder form of residues metal salt and carbonate material from boiling/distillation tap water.

Sintered at 400˚C and 900˚C: at 400˚C and 900˚C

DLS: Diffuse light scattering

XRD: X-Ray Diffraction

SEM: Scanning electron microscopy

EDS: Energy-dispersive X-ray spectroscopy

FTIR: Fourier transformation infrared spectroscopy

BET: Brunauer-Emmett-Teller (BET) Surface Area

BJH: Barrett-Joyner-Halenda (BJH) Pore Size distribution

1. Introduction

Tap water is used for daily life activities like cooking, washing, drinking, and many other household needs. The main source of supply of tap water is lakes, seas, and reservoirs[1]. Survey analysis shows that the tap water that is mostly used in household activities is hard water as it contains $CaCO_3$ above 200 mg/L[2]. Generally, the hardness present in water is of two types: (a) Temporary Hardness and (b) Permanent Hardness. The bicarbonate of magnesium ($Mg(HCO_3)_2$) and calcium ($Ca(HCO_3)_2$) are responsible for causing temporary hardness of water[3]. At high temperature, this bicarbonate further decomposes into calcium carbonate, carbon dioxide and water.

$Ca(HCO_3)_2$ (s) $\rightarrow$ $CaCO_3$ (s) + H_2O (l) + CO_2 (g)

These carbonates are insoluble in water and hence get deposited on various types of heating elements such as a metallic rod, kettle etc[4]. Temporary hardness can be removed by boiling of water. Dissolved chlorides and sulfate of calcium and magnesium are responsible for causing permanent hardness of water[5]. Permanent hardness cannot be removed by boiling. Permanent hardness can be removed by adding precipitating agent which replaces the hardness causing ions. The existence of these ions affects the water in many ways like the destruction of soap and the formation of deposits[6]. At this point, these hardness causing ions are reacts with the hydrophilic part of soap resulting in the deposition of ions takes. As a result "soap scum" is created which tends to decrease the soap's effectiveness and results in the vividness of the clothes[7]. The hardness of water is either measured in grain per gallon or in parts per million (ppm).

Patiala has a Public Authority of Water Supply and Sanitation that plays a major role in supplying tap water to the whole city. Most of the houses get water supply from Bhakra Dam with the help of this authority. The tap water supply in our institute Thapar Institute of Engineering and Technology is come from Bhakra Dam. The tap water is first distilled using double distillation apparatus and then used in our research lab for various chemical reactions. In double distillation apparatus, tap water is boiled at high temperature for five or six hours in the round bottom(RB) flask (5L).The residue left after boiling the water in the RB flask at the bottom is considered as waste and is not utilized further. These residues contain $CaCO_3$ $MgCO_3$, CaO, and SiO_2 compounds. Since, these residues are very cost effective and nontoxic in nature, easily available by the extraction of water from different natural water

sources. These residues are used in various applications like in the production of refractory bricks, cosmetics, paper, paints[8], plastics fireproofing, and fire extinguishing compositions, chalk powder, and toothpaste[9] and also in the area of catalyses like adsorption, degradation, biodiesel formation and photocatalytic applications. Ameta *et.al* **[10]** (2014) examined the photocatalytic degradation of methylene blue via calcium oxide (CaO) as a semiconductor. The impact of different parameters, for example, the concentration of dye, pH, and light intensity has been studied. This photocatalytic process obeys pseudo-first-order kinetics. Zhao M *et.al* [11] (2017) uses the core-shell of $CaCO_3$ as an adsorbent for removal of anionic dyes from solution.$CaCO_3$ microspheres (MSs) were synthesized at room temperature by facile synthesis.

The impact of different parameters, for example, amount of adsorbent, contact time has been studied. These $CaCO_3$ MSs take just 2 minutes to remove 99-100% anionic dye from solution. Han-bing Zhang *et.al* [12] (2017) showed the removal of methylene blue and congo red dye by with $CaCO_3$ (CCB) modified with bentonite. The various parameters were studied for removal of Methylene blue and Congo red dye like SDBS and pH. This CCB Shows their maximum adsorption capacity of MB and CR in range of pH 2~10. The adsorption studied of CCB for CR and MB shows that the process of adsorption was monolayer process**.** NasarMansir *et.al* [13] (2017) synthesis W-Zr \Cao and use as a catalyst for production s biodiesel from FFA waste cooking oil. The reaction of biodiesel was performed at RT, 2wt% catalyst loading, 15:1 methanol to oil ratio, 80˚C temperature for 1 hour. The reaction yield was observed 91.1%. Madhusudhana N[1]*et.al* [14](2012) examined photocatalytic degradation of Violet GL2B azo dye by CaO and TiO_2. The impact of various parameters such as pH, adsorbent dose,and dye concentration has been studied. This CaO shows their maximum degradation capacity of Violet GL2B azo dye at pH 7. Bankovic*et.al*[15] (2017)synthesizednano size CaO to increase its catalytic activity and further was used as a solid catalyst in trans-esterification reaction for conversion of fats and oil to biodiesel. They used a different nanosize catalyst for production of biodiesel like waste material containing CaO, doped and loaded CaO.

Various textile and dye manufacturing industries release their pigment or dye into wastewater. The stability of these dyes toward light, oxidizing agent and heat provides resistance to biodegradation and this creates a lot of problem for species present in water[16]. So, it is very difficult for the industry to handle this enormous amount of dye wastewater to remove toxicity and pollutants[17]. Malachite green is triphenyl methane dye which **is** green in

color. It is used in many industries for giving dying of silk, juice, cotton and wool [18]. Non-biodegradable nature of MG dye affects the environment and human health. The malachite green dye shows its maximum absorbance at wavelength of 616 nm[19].

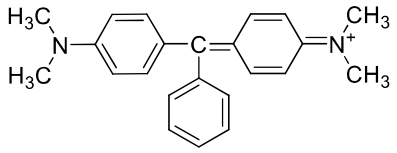

Fig.1: Structure of Malachite Green

Our aim is to extract and characterize RMP-TWB to study its catalytic property. The main objectives are as follows:

- Extraction and characterization of hardness causing material powder from tap water boiling (RMP-TWB).
- Study of its catalytic (dark adsorption) and photocatalytic (degradation) activity.

2. Materials and Methods

2.1 Materials

Ethanol, methanol, Distilled water were purchased from Loba Chemie India and Malachite green dye were purchased from Loba Chemie India, Residues RMP-TWB as adsorbent were extracted from TWB.

2.2 Method of Extraction RMP-TWB

Hardness causing residues RML-TWB of carbonates from boiling/distillation tap water (TWB) were taken and then these residues are centrifuged (8000 rpm, 5 min, 25°C) and three times wash with water, ethanol respectively. Later it was dried at room temperature. The powder form of residues (RMP-TWB) is further sintered at 400°C and 900°C for 4 hours in the furnace. The powder form of residues (RMP-TWB) is further sintered at 400°C and 900°C to characterize its properties.

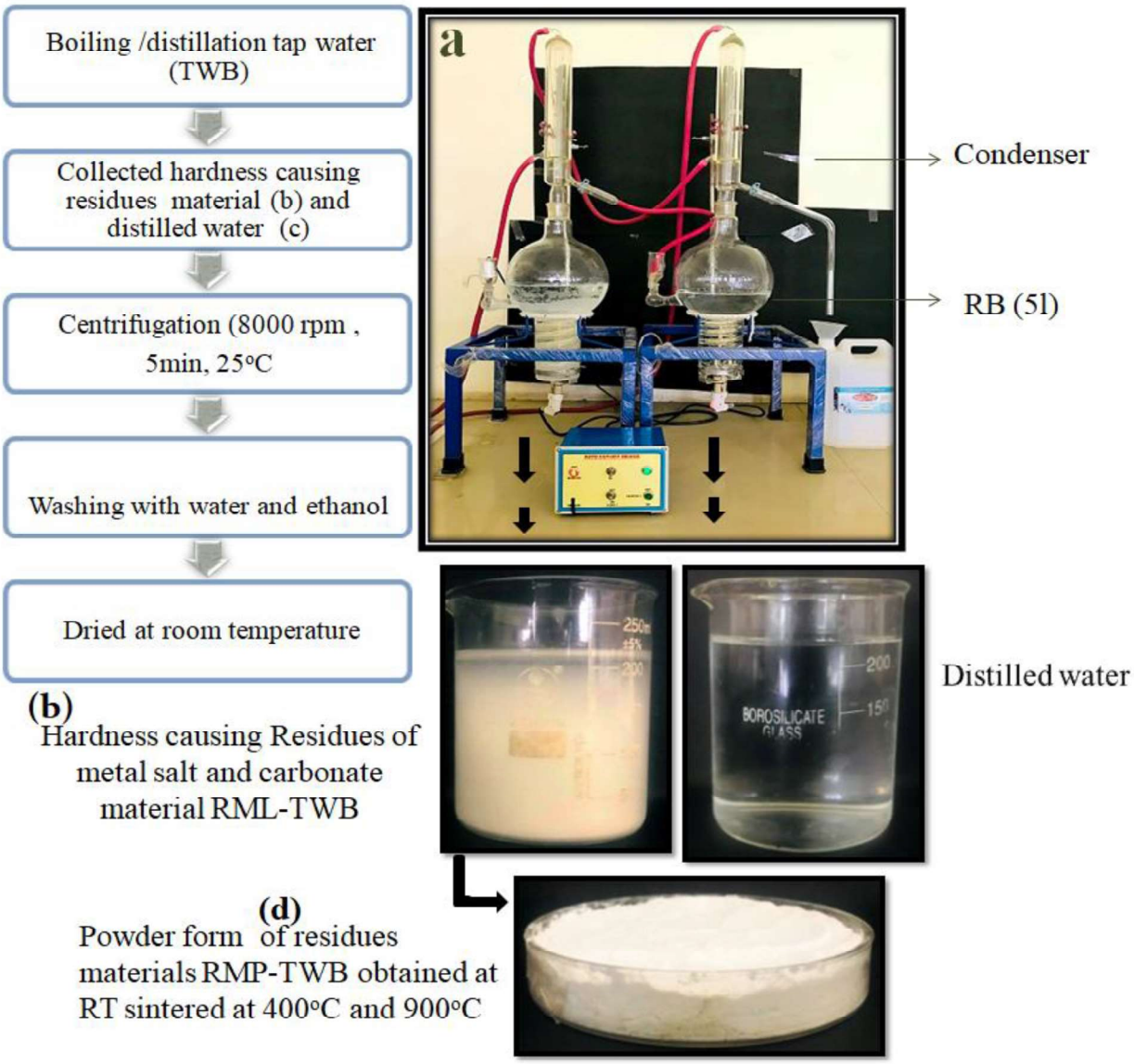

Scheme 1: Extract of hardness causing residues RMP-TWB from boiling/distillation tap water (TWB).

2.3 Characterization techniques

In this work we have used a variety of characterization methods to study the surface morphology; composition and surface area of RMP-TWB so the techniques are used in this experiment.

Dynamic light scattering technique is used to determine the particle size or average size distribution in solution. The hydrodynamic size of RML-TWB and RMP-TWB obtained at

RT and sintered at 400ºC, 900ºC was determined by Malvern ZEN3600 particle size analyzer.

X-Ray crystallography is used to determine the structure and size of crystal (organic chemical compound. The structure and size of the crystal of RMP-TWB obtained at RT and sintered at 400^0C 900^0C was determined by PAN analytical- Xpert High score with a diffraction angle of 20-90˚ at 5˚ rise/min.

Scanning Electron microscope (SEM) is used to determine surface morphology and size of RMP-TWB. We used JSM-7600 F (0.1 to 30 KV) Instrument in SAI labs (Thapar University, Patiala) for analysis the surface morphology of RMP-TWB in SAI labs (Thapar Institute of Eng, and Technology, Patiala).

FTIR used to study the structure of the different chemical group present in a molecule and also detects the functional group present in a molecule. The functional group present in residues RMP-TWB is identified by (Agilent technology) FTIR spectroscopy.

UV visible spectroscopy is used to find the concentration of different molecules in solution or used to find the concentration of the color solution (dye) at a different time. The optical analysis of RMP-TWB and sintered at 400ºC, 900ºC was analysis by using (Agilent technology) Double-beam UV-Vis spectrophotometer over the wavelength 200-800nm.

BET and BJH are used to calculate the surface area and pore size distribution of RMP-TWB. The Porosity and surface area were studied by BET surface area (BEL mini-Japan).

2.4 Dark adsorption behavior of RMP-TWB

A solution of different concentration (0.2 to 1 mg) of RMP-TWB for the same concentration (0.2 mM) and volume (15 ml) of the dye (0.2mM) was prepared followed by stirring for 15 min in the dark. Centrifugation (8000 rpm, 5 min, and 25ºC) of this solution was done and then analyzed by UV- Visible spectra. In the subsequent experiment, 0.5 mg of RMP-TWB was taken by varying the concentration (0.2 to 0.025 mM) and volume (15 ml) of dye and the same procedure was followed. In the next experiment 1 mg, RMP-TWB was taken for 0.2 mM of dye and the activity of these residues at different temperature (RT, 400ºC, and 900ºC) was compared with commercial CaO and the same procedure was followed.

2.5 Photocatalytic degradation of MG dye

Firstly 0.5 and 1 mg RMP-TWB residue was weighed and added to the 5 ml dye (0.2 mM) in two test tubes. Stirred on a magnetic stirrer for 5 min in dark then centrifuged the solutions

and absorbance value was noted at a specific wavelength. A similar setup is used for degradation of MG under sunlight irradiations for same amount RMP-TWB and concentration of dye as you seen in figure18. Control experiment was also performed by varying the volume from 5 ml to 15 ml and time from 30 min to 15 min figure19. Finally, 0.5 mg and 1mg RMP-TWB were taken in same 30 ml volume of dye (0.2mM) and stirred on magnetic stirrer under sunlight at a regular interval of time 10, 20, 30, 40, 60, 90 min respectively. Change in UV-Visible spectra of MG dye and color transformation from blue to transparent was observed as you shown in figure 20 and 21.

3. Result and discussion

3.1 Optical and Structural characteristics

The particle size distribution of RML-TWB (2 ml) and RMP-TWB at room temperature, 400ºC, and 900ºC were obtained by dispersing 1 mg in 2 ml water followed by the ultrasonic treatment for 30 min. The observed hydrodynamic size (Fig.2, 3) for RML-TWB anRMP-TWB at room temperature, 400ºC, and 900ºC were found to be 1.6µm, 163 nm, 234 nm, and 726 nm respectively.

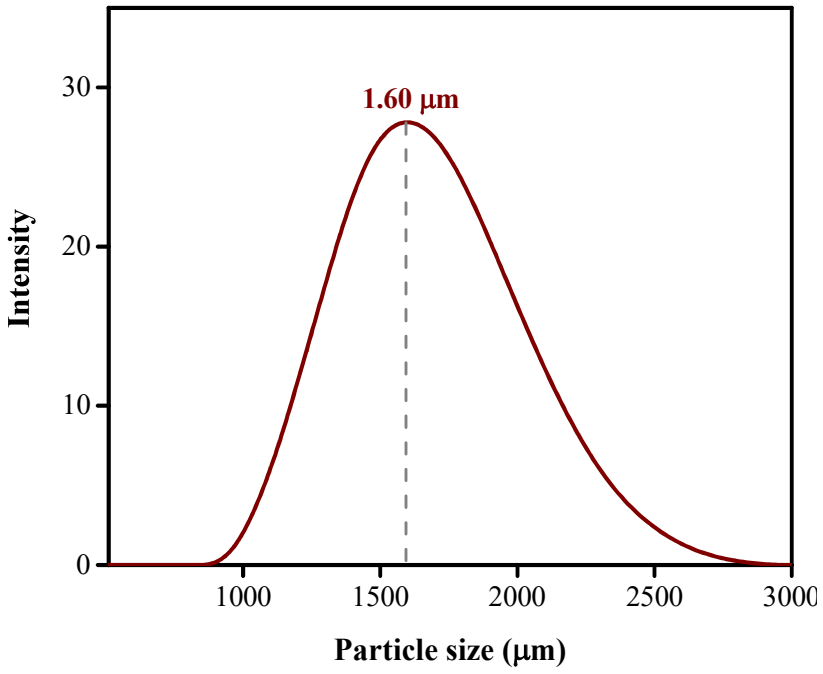

Fig.2: DLS particle size distribution of RML-TWB (2 ml) dispersed in water.

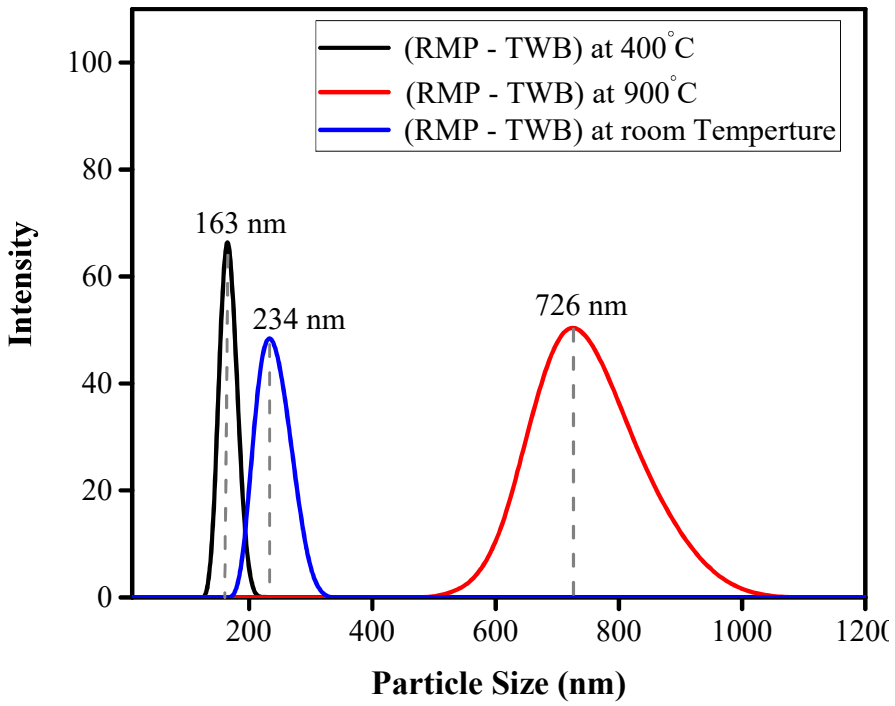

Fig.3: Diffuse light scattering (DLS) particle size distribution of powder (RMP-TWB) obtained after 5-6 h boiling tap water (TWB) and sintered at 400ºC and 900ºC.

Composition and crystalline form of the element present in RMP-TWB was identified by XRD. Fig. 4 shows the XRD spectra of RMP-TWB at room temperature and sintered at 400ºC and 900ºC. It was observed that RMP-TWB contains a different element like $CaCO_3$, MgO, SiO_2, Mg_2 (SiO_4) in different crystalline form. The RMP-TWB at room temperature shows high intensity peaks at diffraction angle 26.21º,27.20º,36.14º,45.78º,48.25ºand50.19º corresponding to plane (111), (021),(102),(221),(041),and (132) of $CaCO_3$ (JCPDS Card no.01-075-2230), & less intensity peak at 52.40º, 59.15º, 75.55º,79.08º and 82.32º known with this plane (113), (311), (204), (243) and (162) of ($CaCO_3$ (JCPDS Card no.01-075-2230).The peak of MgO (JCPDS Card no.01-075-0441) at diffraction angle 42.86° corresponding to (200) plane and similarly Peak of SiO_2 (JCPDS Card no.00-047-1300) at diffraction angle 33.12° related to (212).

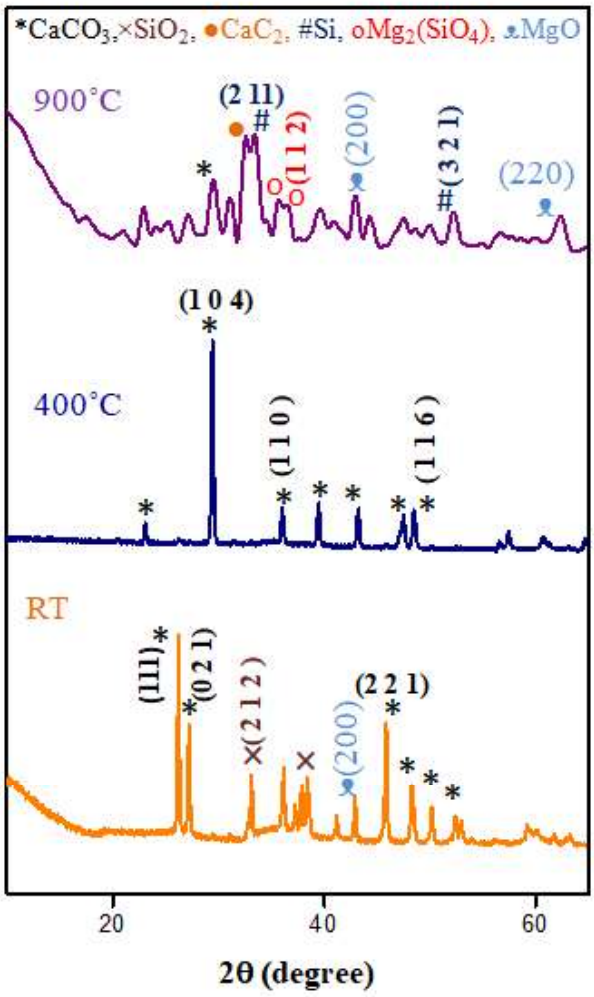

Fig.4: X- Ray Diffraction (XRD) pattern of RMP-TWB at room temperature and sintered at 400ºC and 900ºC.

The high-intensity peak of RMP-TWB of 400ºC at diffraction angle 2Θ are 29.36º, 35.99º, 39.45º, 43.15º and 48.45º corresponding to different plane (104), (110), (113), (202) and (116) & less sharp peak at 47.46º, 57.45º and 60.67º identified with this plane (018), (122) and (214). This all peak of diffraction corresponding to the different plane at 2Θ exactly matches the report XRD spectra of $CaCO_3$ (JCPDS Card no.01-086-0174) [20]. While, the high intensity peak of RMP-TWB of 900ºC observed at 22.87º,29.39º,32.32º,33.38º,36.46º,42.88º and 52.27º are related to different plane (021), (104), (110), (221), (112), (200) and (321) & less sharp peak at 23.82º, 27.21º, 47.50º and 62.36º identified with planes (211),(011),(018) and (220). These peaks of diffraction at a specific angle for the particular arrangement is related to these chemical compound like MgO (JCPDS Card no.00-045-0946), $CaCO_3$

(JCPDS Card no.01-081-2027), SiO_2 (JCPDS Card no.01-078-1259), Mg_2 (SiO4) (JCPDS Card no.01-080-0944), Si (JCPDS Card no.01-079-0613)[21].By analysis the XRD data, it was revealed that at RT maximum amount of $CaCO_3$, SiO_2 present in RMP-TWB. On increasing the temperature $CaCO_3$ decomposes into CaO and CaC_2, SiO_2into Si and some amount of undecomposed $CaCO_3$ was also present.

The surface morphology and size of residues of RMP-TWB was confirmed by scanning electron microscopy. Fig.5 shows the SEM images of RMP-TWB at room temperature which shows the rod shape of RMP-TWB and the range of particle size lies between from 1µm to 10µm.Similarly, Fig.6 shows the SEM images of RMP-TWB at 400ºC which shows the sphere and rod shape of RMP-TWB and the size of particles lies between from 1µm to 10µm. Fig.7 shows the SEM images of RMP-TWB at 900ºC which shows the anisptropic sphere like shape of RMP-TWB and the size of particles lies between from 1µm to 10µm.

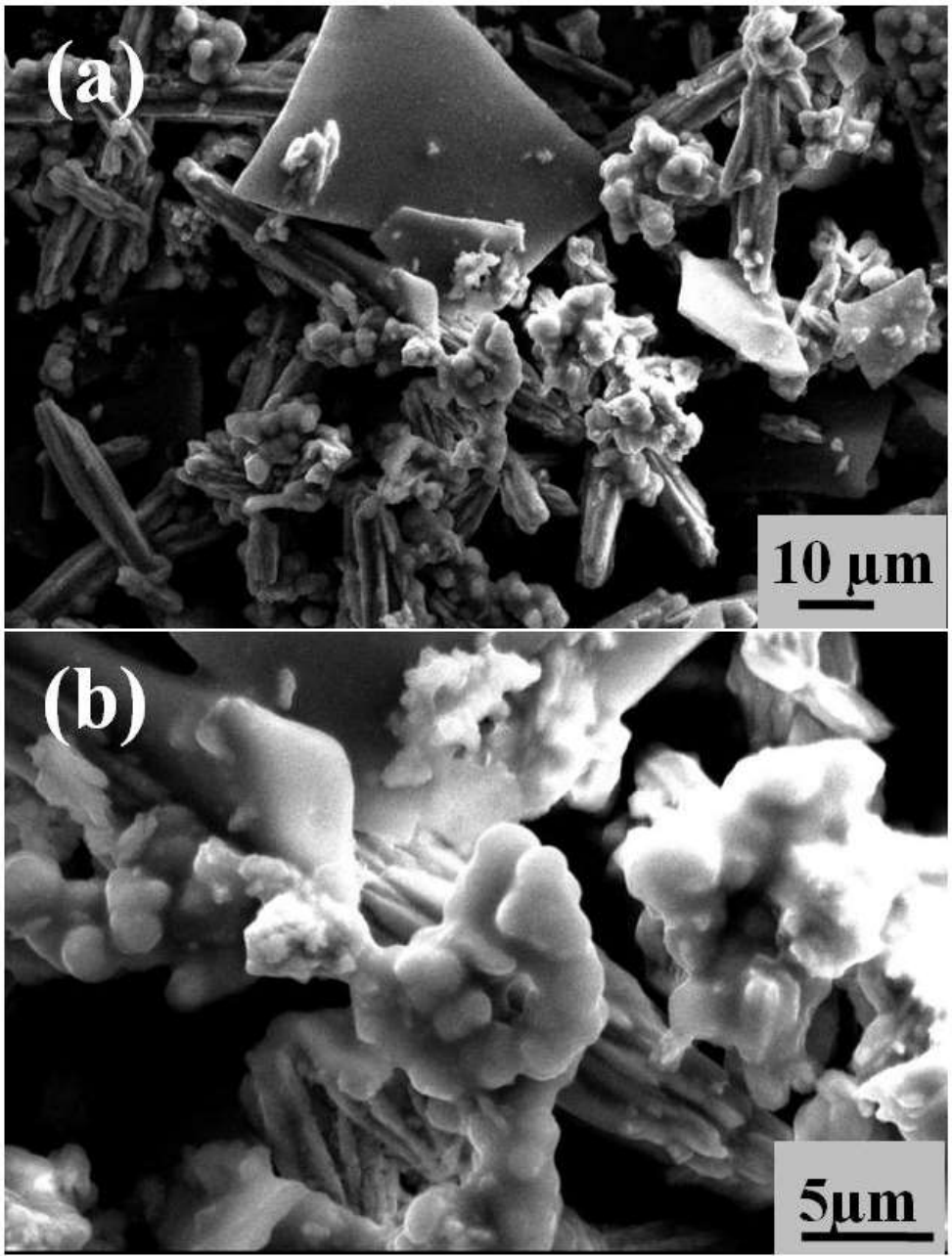
(a)
10 µm
(b)
5µm

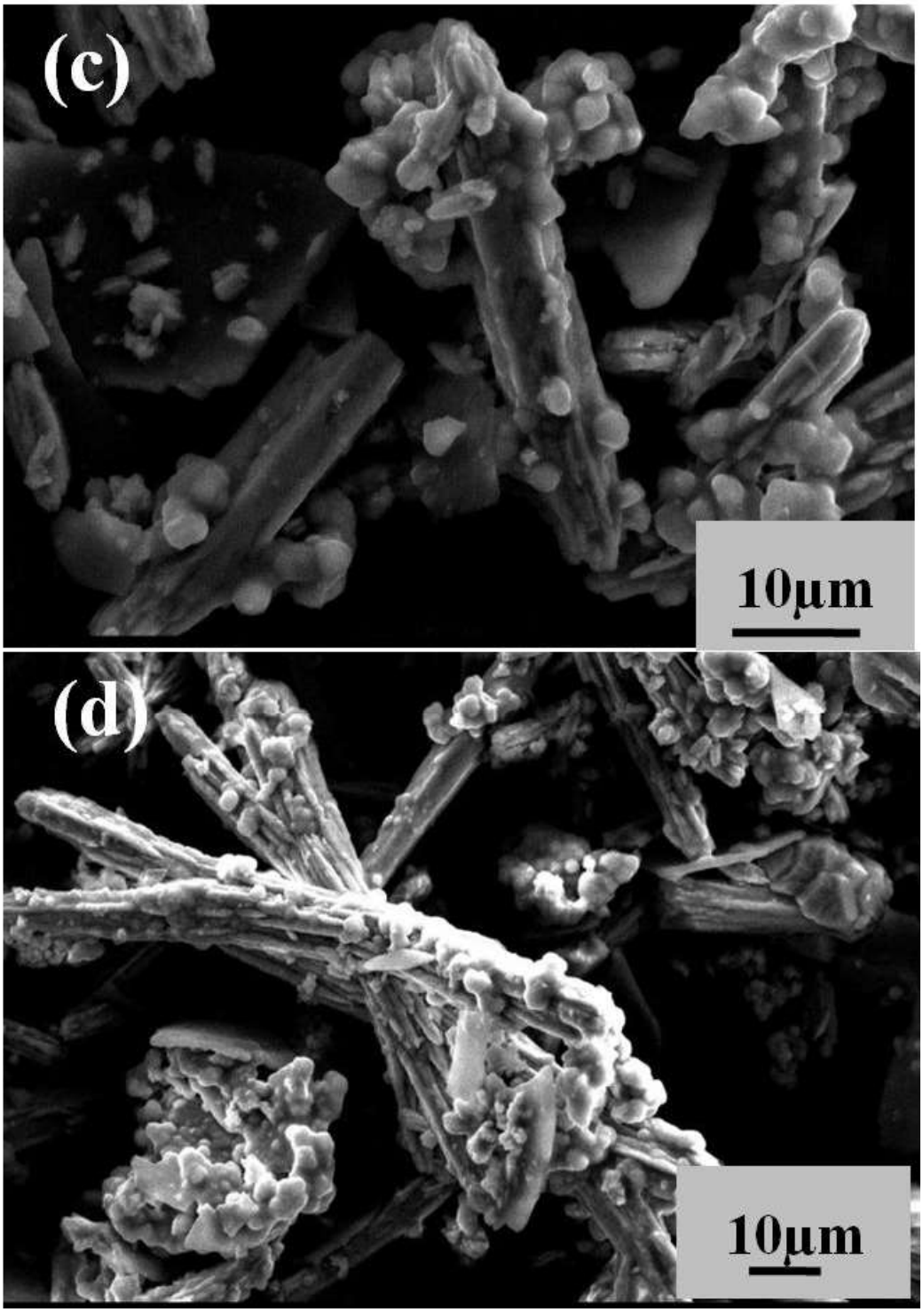

Fig.5: SEM images of RMP-TWB obtained at room temperature.

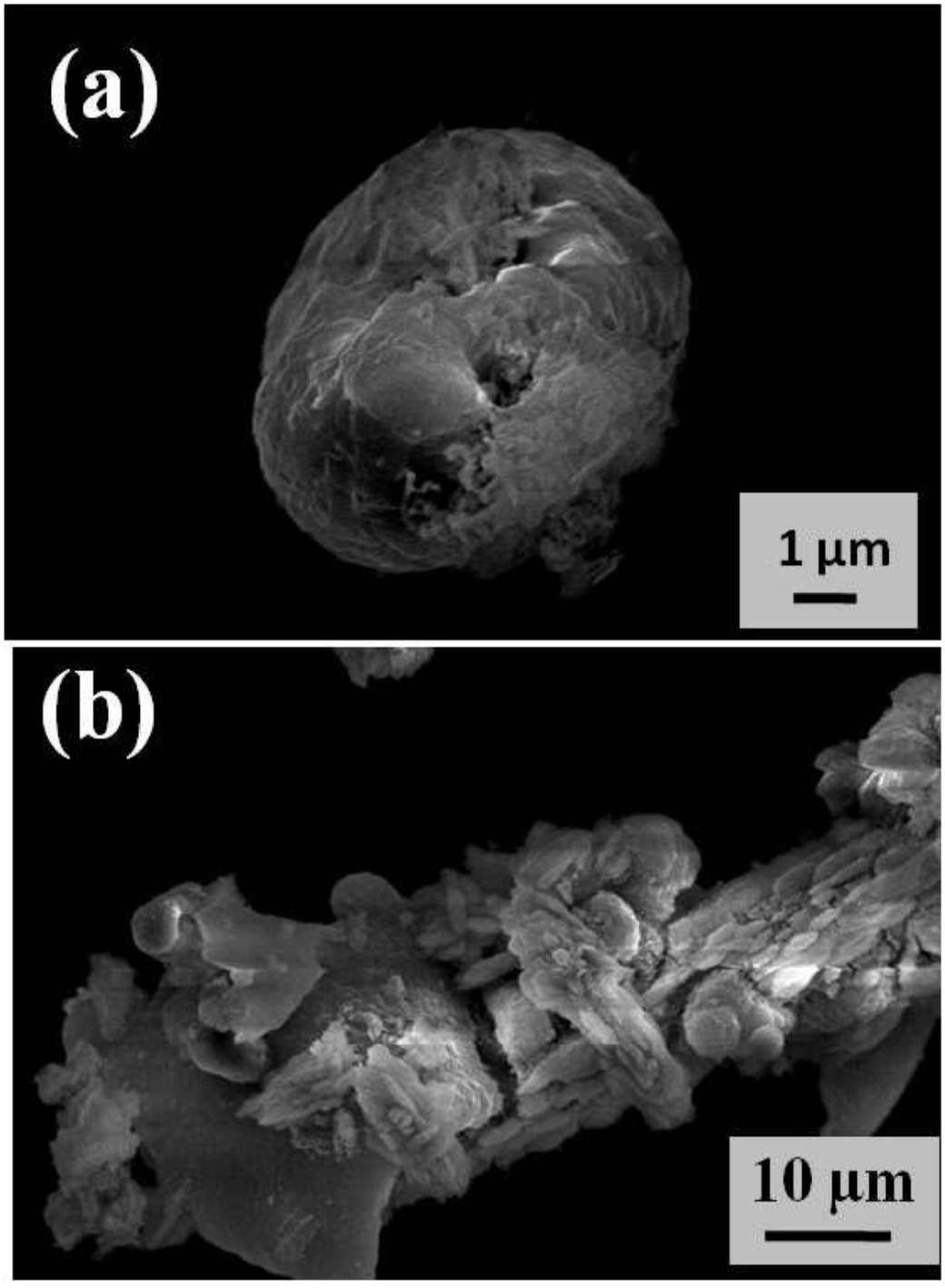
(a)
1 µm
(b)
10 µm

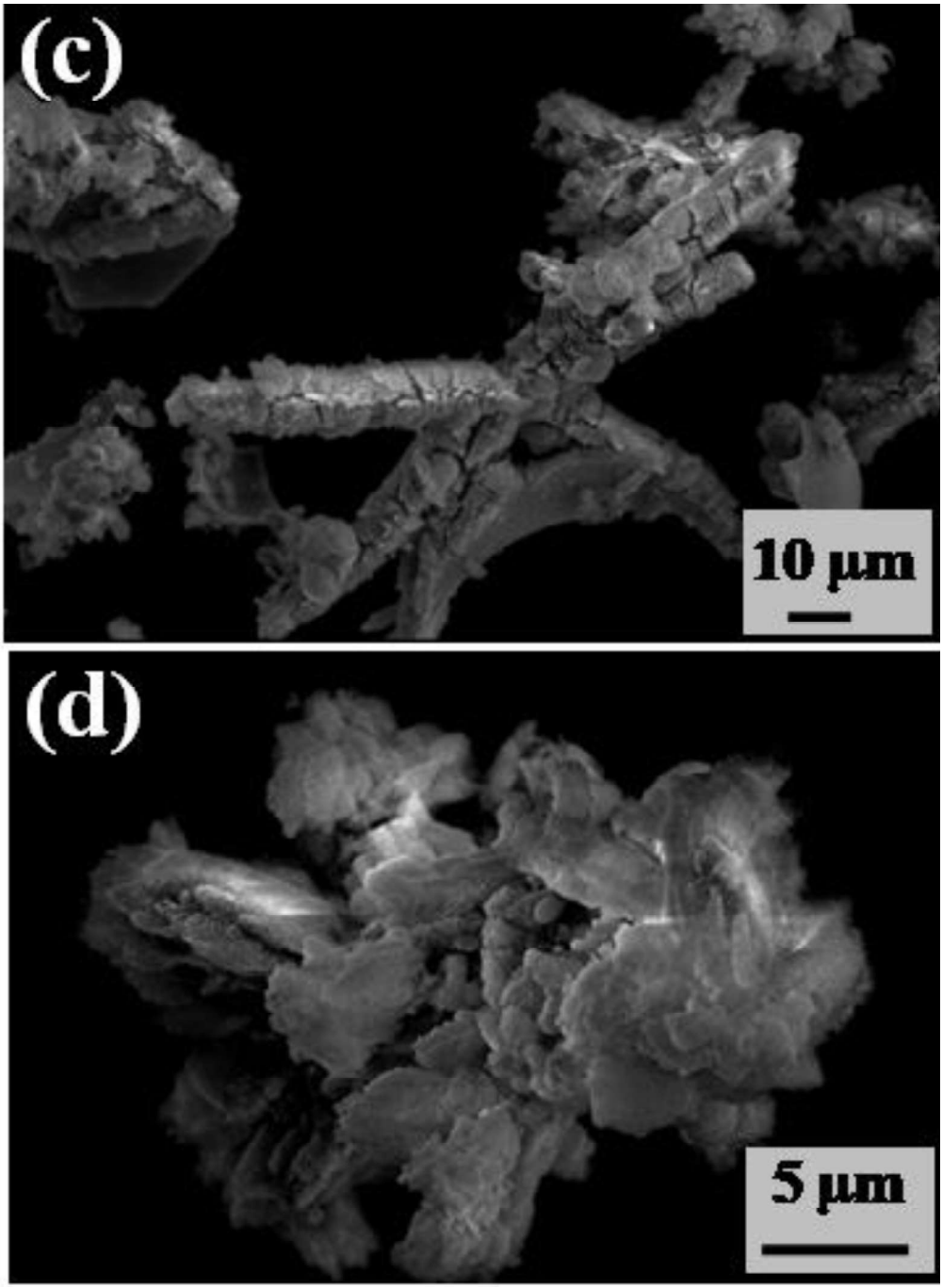

Fig.6: SEM images of RMP-TWB sintered at 400ºC.

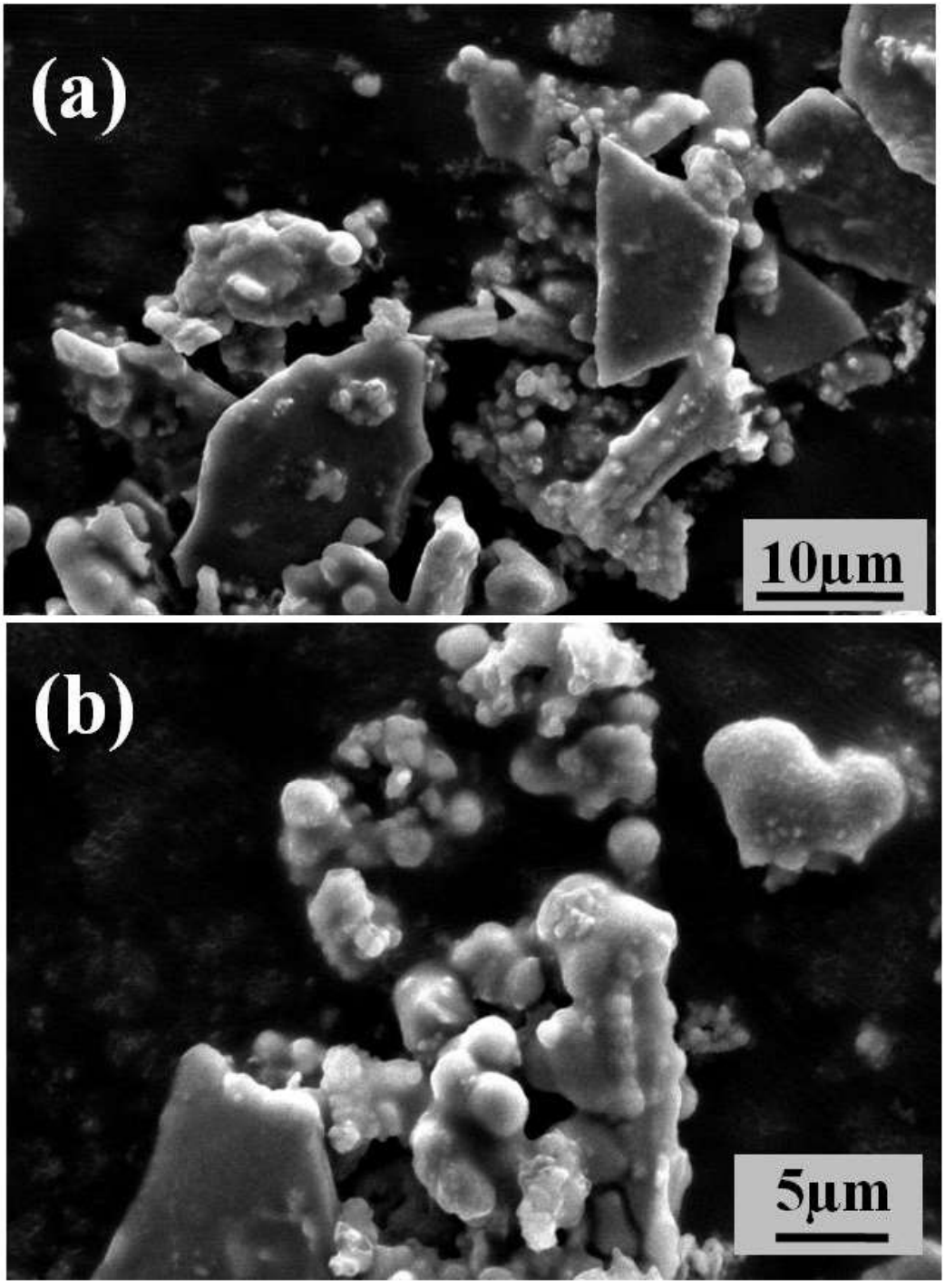
(a)
10µm
(b)
5µm

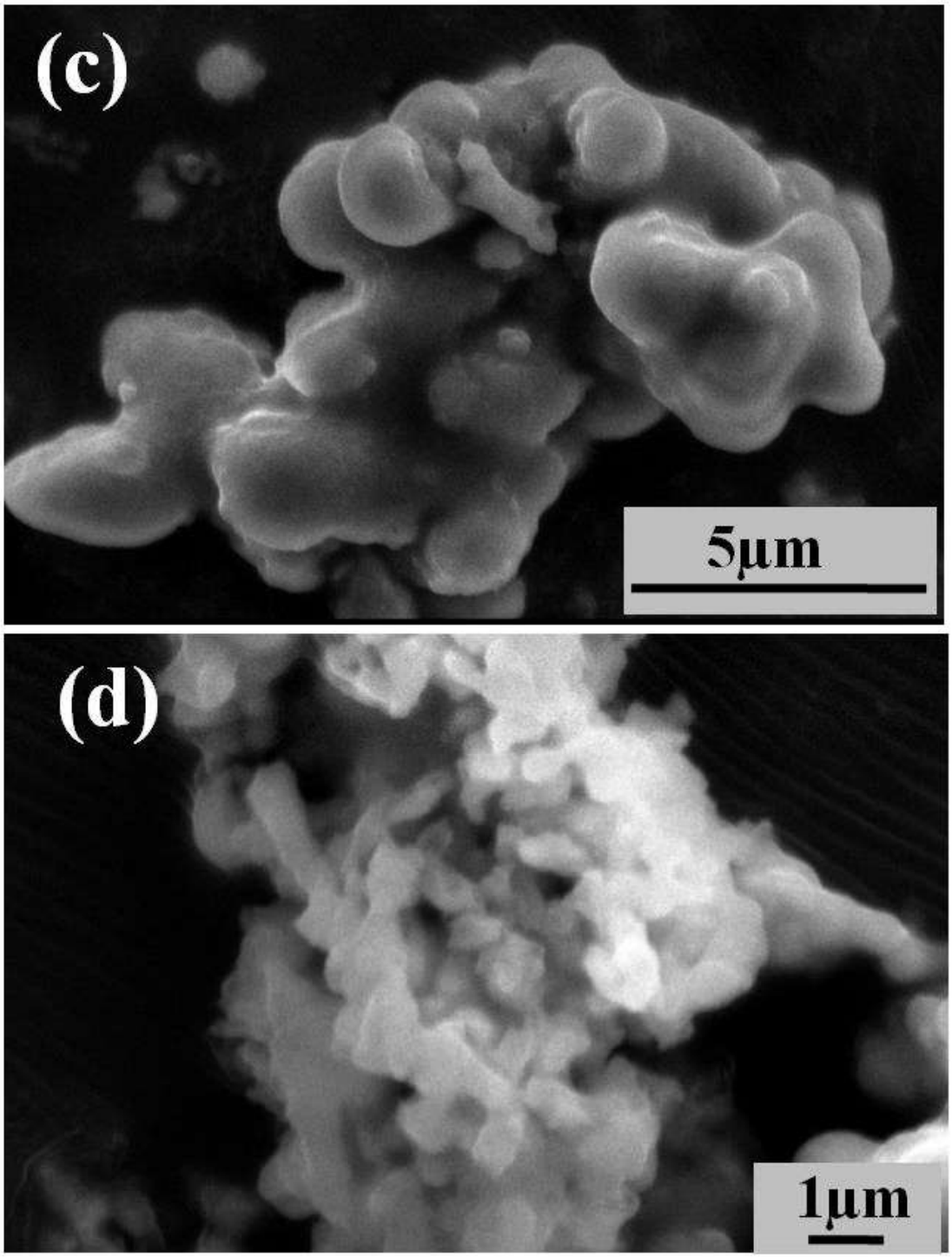

Fig.7: SEM images of RMP-TWB sintered at 900ºC.

The EDX analysis tells about the element present in RMP-TWB and element mapping gives the different color to the different elements. The figure 8 shows that the elements like C, O, Mg, Ca and Si are present in RMP-TWB which was also confirmed by XRD.

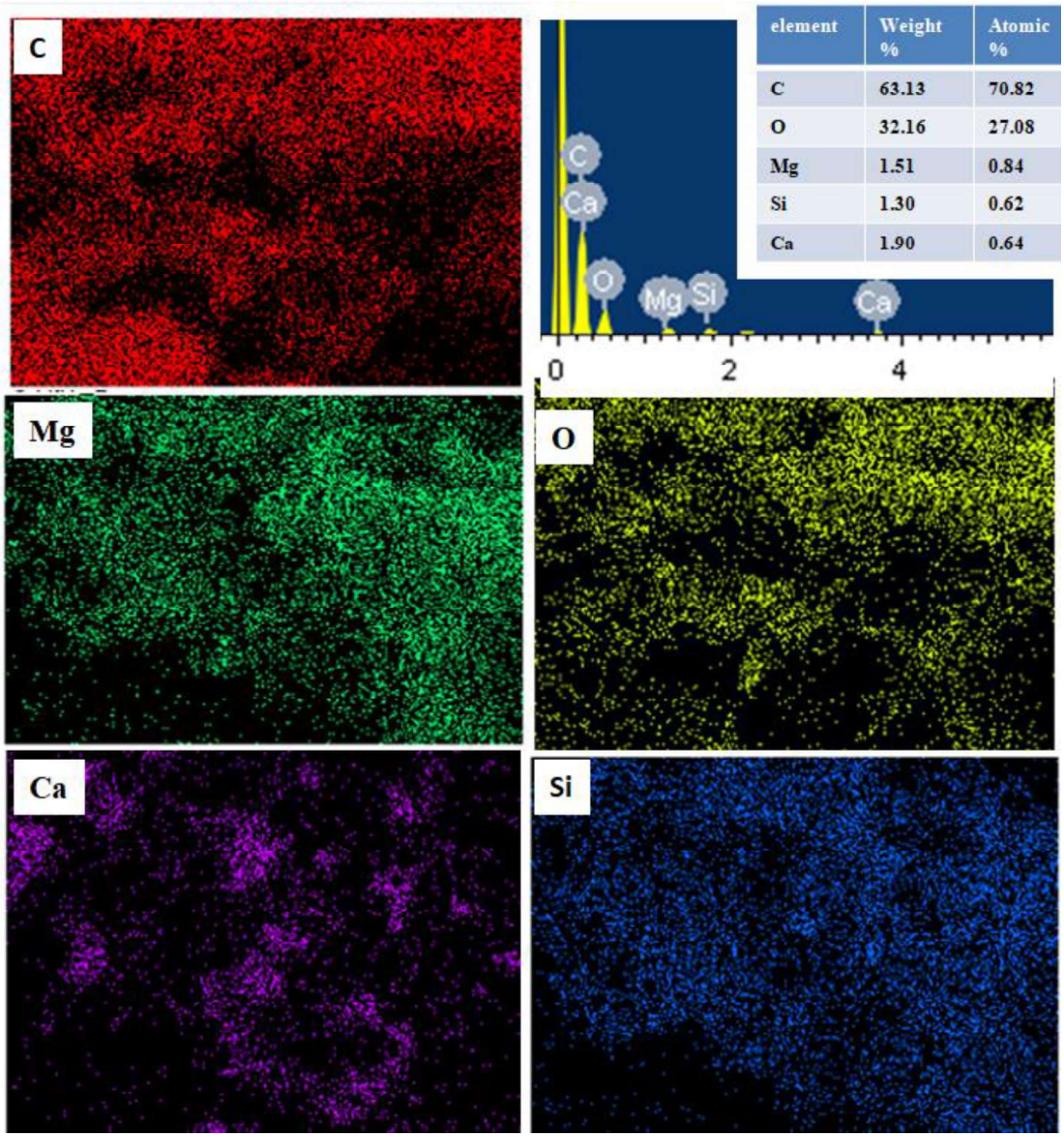

element	Weight %	Atomic %
C	63.13	70.82
O	32.16	27.08
Mg	1.51	0.84
Si	1.30	0.62
Ca	1.90	0.64

Fig.8: Element mapping and Energy-dispersive X-ray spectroscopy (EDS) analysis of RMP-TWB.

Fig.9 shows the absorption bands of residues RMP-TWB arise due to presence of different functional groups. FTIR spectra of RMP-TWB at room temperature and 400ºC shows three similar absorption bands at 640 cm^{-1}, 946 cm^{-1}, 1424cm^{-1} and 2361 cm^{-1}. These peak arises

due to symmetric and unsymmetrical vibration of CO^{3-} ions[22] and harmonic vibration of Ca-O. The absorption band from 2600 to 3600 cm^{-1} is due to stretching vibration of O-H.

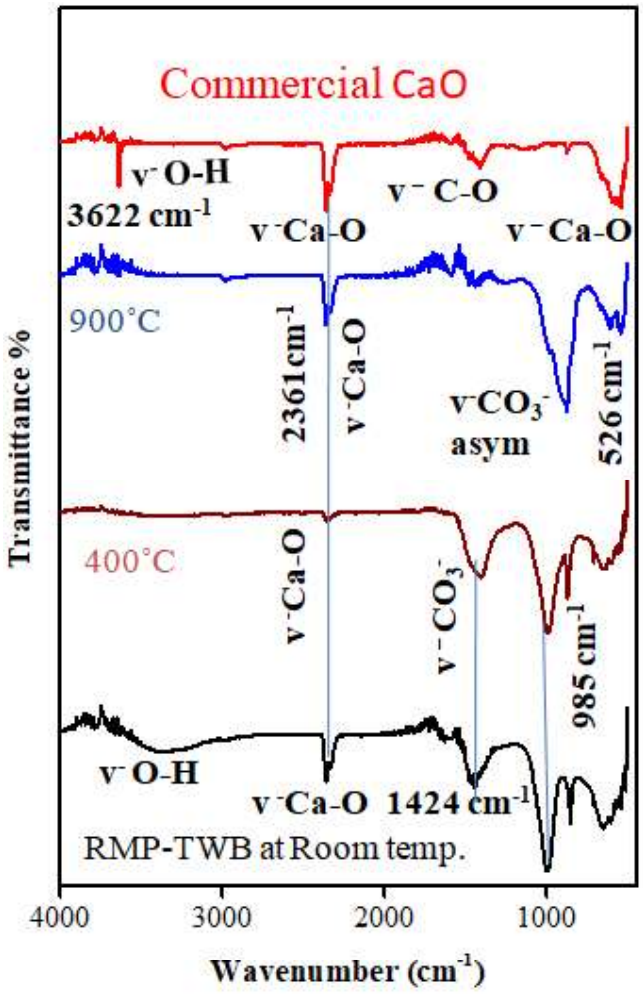

FTIR spectra of Commercial CaO and RMP-TWB at 900ºC shows absorption band of 545cm^{-1} and 2361 cm^{-1} because of symmetric and harmonic vibration of Ca-O. The absorption band at 3622 cm-1 is due to stretching vibration of O-H. This FTIR spectrum of RMP-TWB and commercial CaO exactly matches with the reported FTIR spectra for $CaCO_3$ and CaO [22].

For analysis, the adsorption and photocatalytic degradation of dye, surface area and pore size distribution of RMP-TWB residues are very important property. The surface area of RMP-TWB residues are analysis by BET isotherm and Pore Size Distributions. The figure10 (a) shows the Nitrogen adsorption and desorption isotherm of RMP-TWB. The surface area of RMP-TWB is 35.4 m^2g^{-1} and mean pore diameter 10.08 nm.

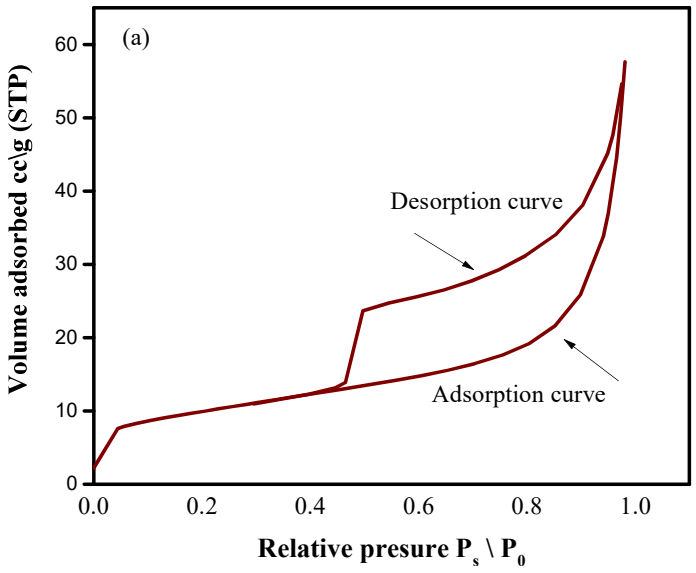

This Nitrogen adsorption and desorption isotherm of RMP-TWB resemble with class IV type which is accounted for mesoporous material. At moderate pressure, this curve is corresponding to the monolayer- multilayer adsorption. When the relative pressure reaches above 0.90 there is an abrupt increase in the isothermal curve which is because of capillary condensation and range of size in mesopore to macropore[23]. There is a condensation occurring during adsorption process which filled the vacant pores of the surface with the liquid. In comparison, evaporation occurs during desorption process.

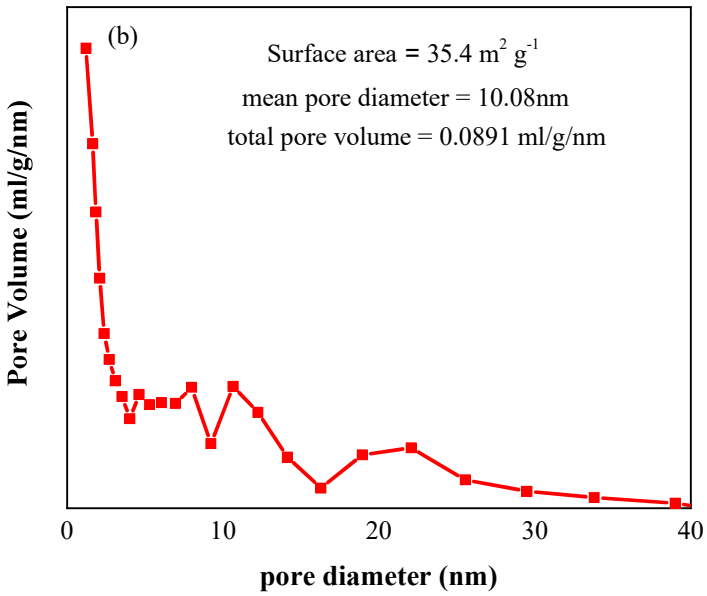

Fig.10: (a) BET surface area isotherm (b) BJH curve of RMP-TWB sample obtained at room temperature.

Pore size distribution of RMP-TWB is analyzed by BJH method. Figure 10 (b) shows the BJH curve of RMP-TWB sample obtained at room temperature. Pore size distribution of residues RMP-TWB mean pore diameter 10.08 nm[23].

3.2. Calibration graph of malachite green dye

To study the dark adsorption and photocatalytic degradation of MG dye first we make calibration graph of MG. we make solution of different concentration of dye like 0.2, 0.15, 0.1, 0.05, 0.025 mM. These solution prepared by taking 0.014 g in 200 ml of water in 200 ml beaker. The absorbance of each dye solution was measured with double beam UV visible spectrophotometer and calibration graph between absorbance vs. concentration was plotted.

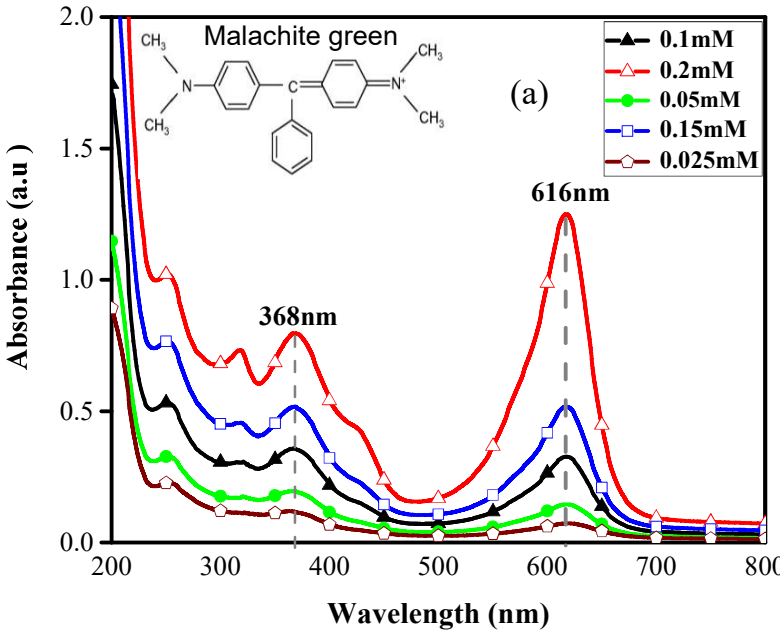

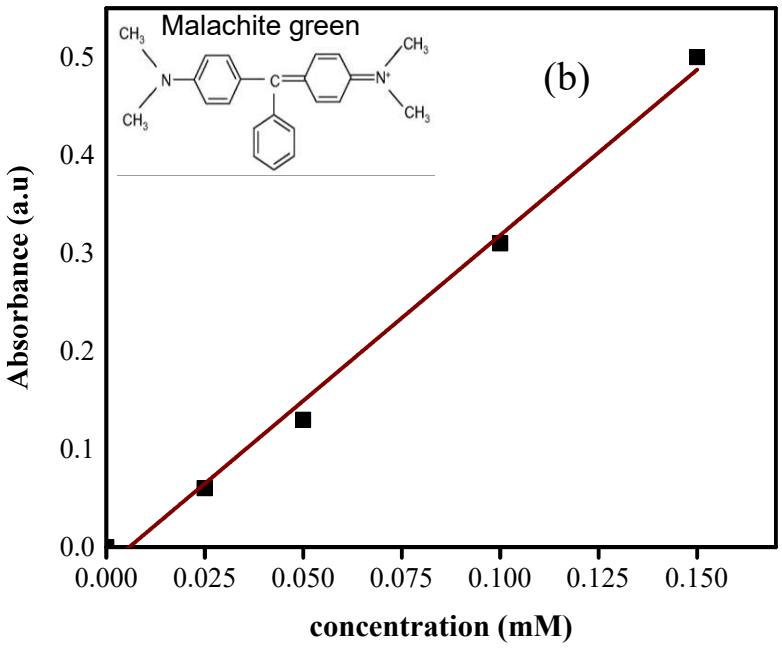

Fig.11: (a) Absorbance spectra and (b) Calibration graph (absorbance vs concentration) of malachite green dye.

3.3. Section A: Dark adsorption

Figure 12 shows the dark adsorption of MG dye (0.4Mm 0.3mM) but the value of absorbance observed was very high so it doesn't follow beer lamberts law.

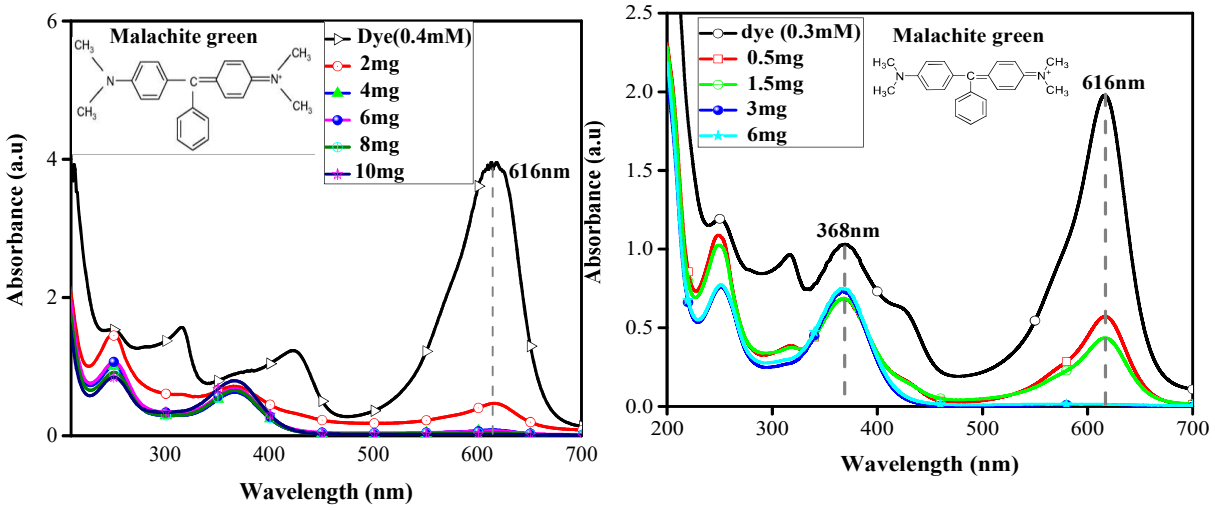

Fig.12: Effect of different concentration of MG dye and RMP-TWB sample on adsorption of dye and changes their color intensity.

Figure 13 shows the effect of the amount of RMP-TWB on adsorption of MG[24]. It is clearly seen that the amount of RMP-TWB increases from 0.2mg to 1mg, the availability of active sites on the surface, which increases the extent of adsorption. Table1 summarized the extent of adsorption with a change in the amount of RMP-TWB.

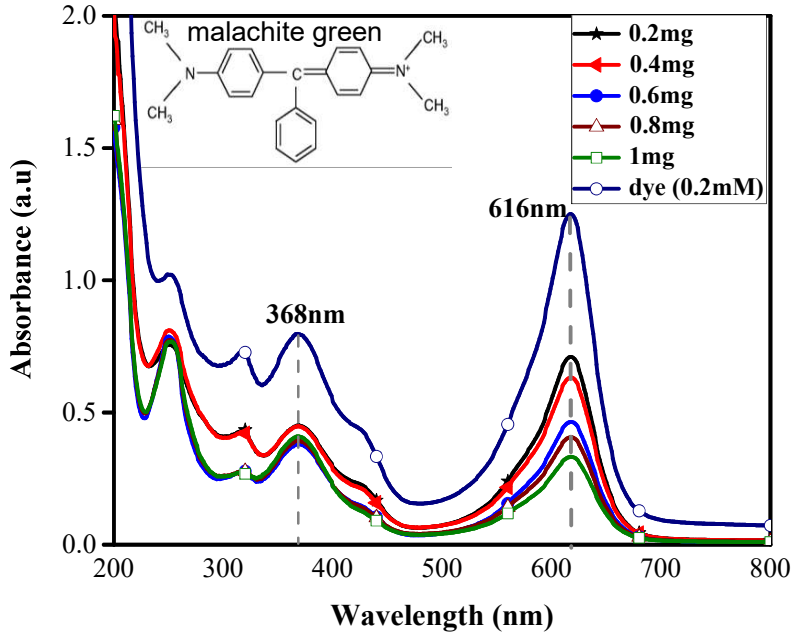

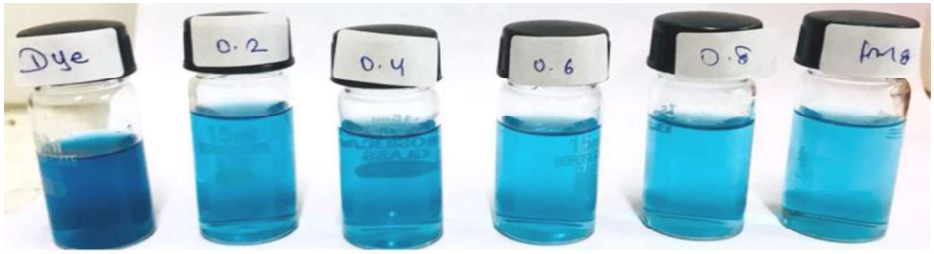

Fig.13: Influence of different amount (0.2 to 1 mg) of RMP-TWB sample on adsorption of MG dye (0.2 mM, 15 ml) and changes in color intensity.

(RMP-TWB) m (mg)	x_i (mg)	x_f (mg)	Adsorbed $x = x_i - x_f$	(RMP-TWB) (mg/ml)	x / m	Volume (ml)
0.2	1.094	0.788	0.306	0.013	1.530	15
0.4	1.094	0.552	0.542	0.026	1.355	15
0.6	1.094	0.394	0.700	0.040	1.166	15
0.8	1.094	0.339	0.755	0.053	0.943	15
1	1.094	0.273	0.821	0.066	0.821	15

Table .1 Variation in adsorption of MG with a change in the amount of RMP-TWB.

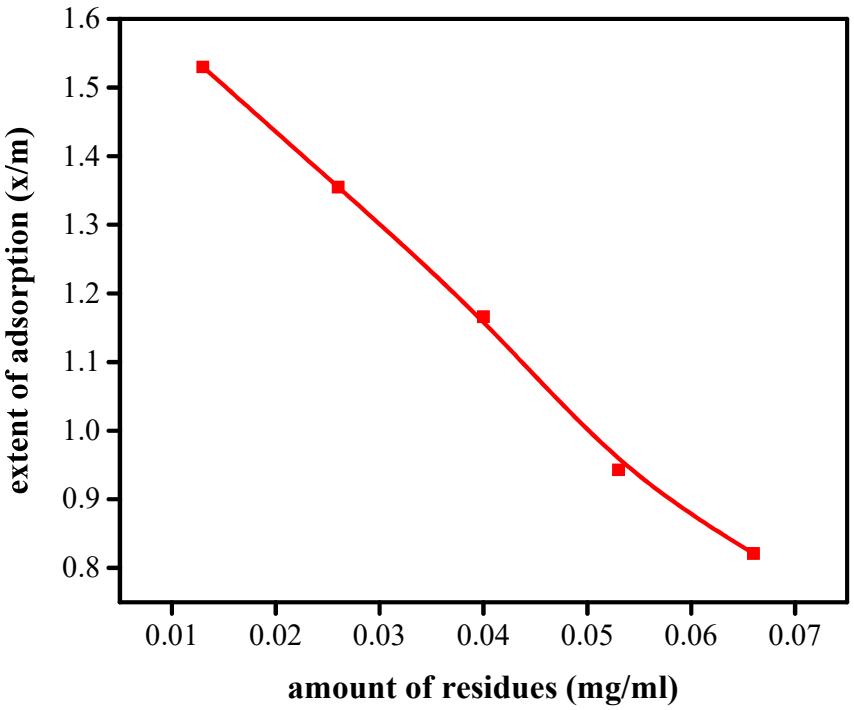

Fig.14: Variation in adsorption of MG dye with amount of RMP-TWB.

The Fig 14 shows that variation in adsorption of MG dye with amount of RMP-TWB.

Fig 15 shows the effect of dye concentration on adsorption of MG. It was observed that as the concentration of dye decrease from 0.2mM to 0.05mM, adsorption of MG dye decrease.

It is because less number of dye molecules is available for adsorption with decrease its concentration, which decreases the adsorption of MG dye.

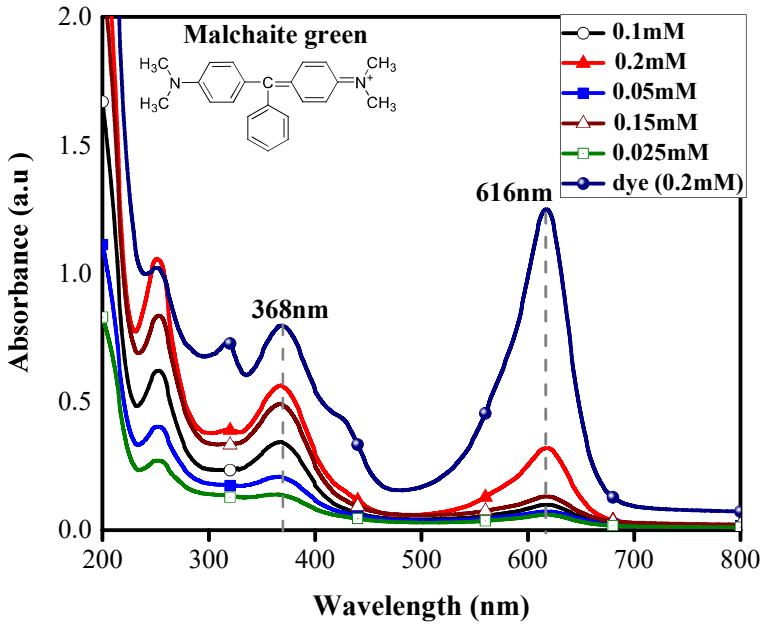

Fig.15: Effect of MG dye concentration and observe colors transformation from blue to transparent.

(RMP-TWB) m (mg)	x_i (mg)	x_f (mg)	Adsorbed $x = x_i - x_f$	log x_i	log x / m	Volume (ml)
0.5	1.094	0.268	0.826	-0.698	0.218	15
0.5	0.821	0.197	0.624	-0.823	0.096	15
0.5	0.547	0.158	0.389	-1	-0.109	15
0.5	0.273	0.125	0.148	-1.301	-0.528	15
0.5	0.136	0.114	0.022	-1.602	-1.356	15

Table 2: Freundlich Adsorption isotherm at different concentration of MG dye

The figure 16 shows that the Freundlich fitting curve for MG dye adsorption. Freundlich Adsorption isotherm $x/m = k\, c^{1/n}$ where x is the amount of adsorbent, m is mass of adsorbent and C is the concentrate of adsorbate and the values of n and K are find by slope and intercept. The value of n>1 shows the Favorable condition for Freundlich Adsorption

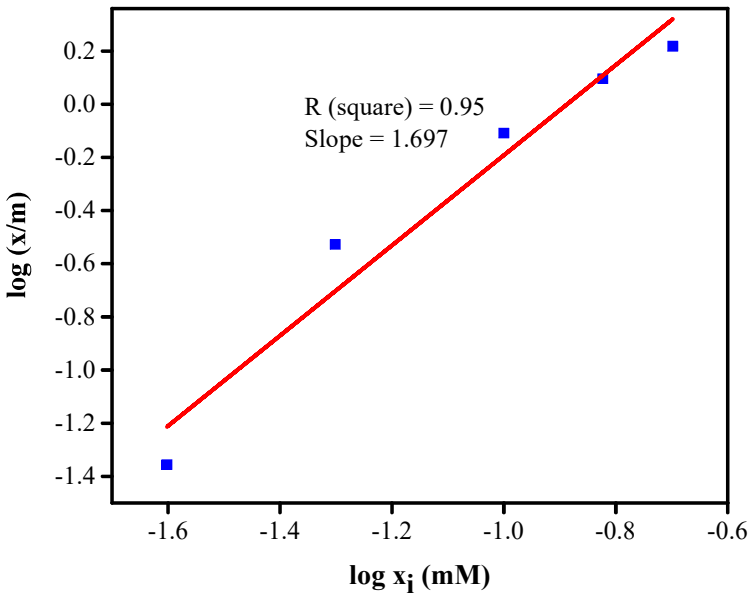

Fig.16: Freundlich Adsorption isotherm at different concentration of MG dye.

Figure 17 Depicts that as the temperature of RMP-TWB was increased RT to 900°C more activity was observed for adsorption of MG.

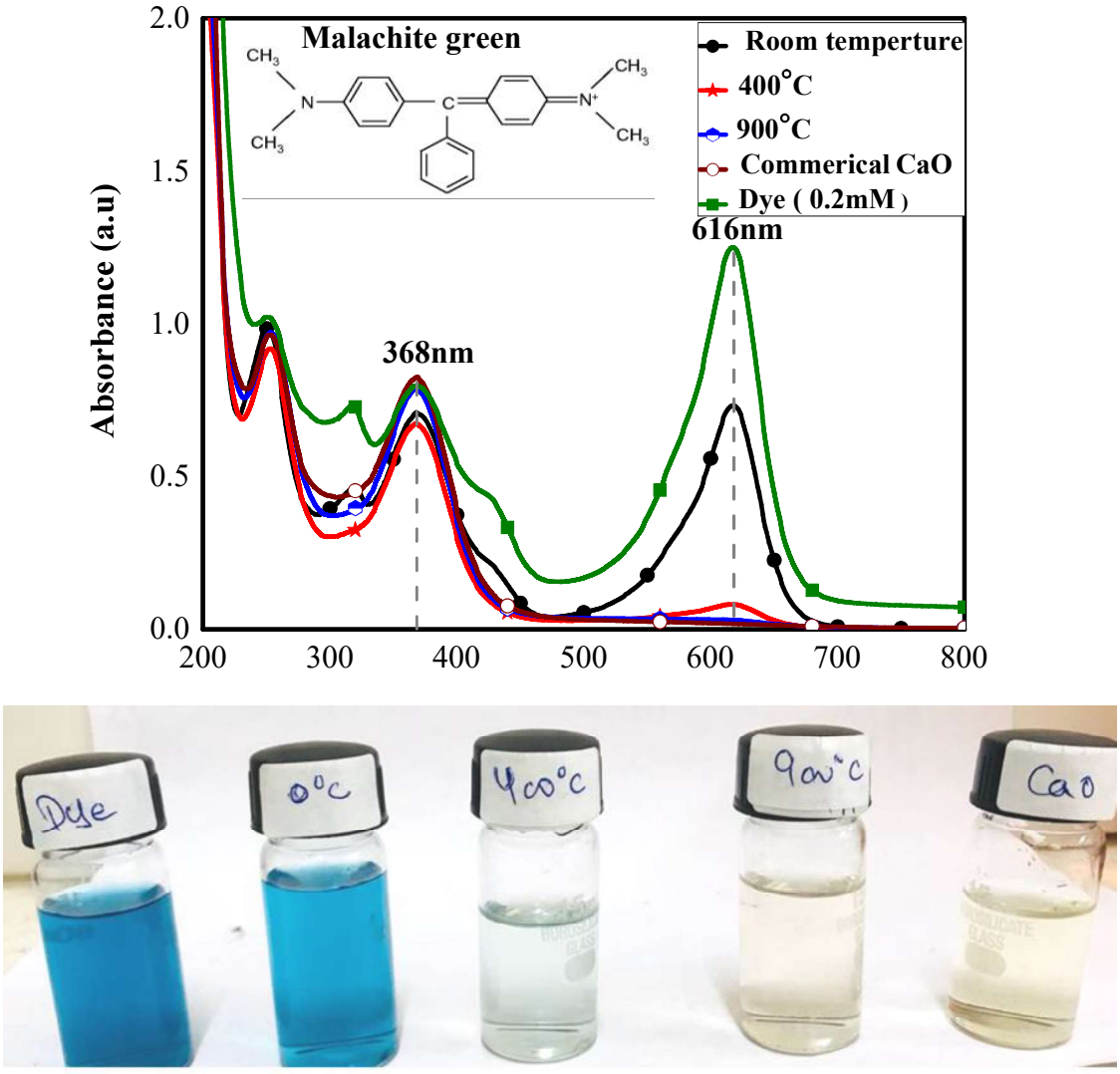

Fig.17: Comparative study of (RMP-TWB) with commercial available CaO at various temperature and observed color transformation from blue to transparent.

3.3. Section B: Photodegradation of MG dye

The literature data concludes that $CaCO_3$, CaO act as a semiconductor for the degradation of MG dye [25]. Characterization data confirms the presence of $CaCO_3$, CaO, and MgO in RMP-TWB. So this motivated us to examine its photocatalytic activity. To see the effect of a catalyst on the degradation of MG with time, 0.5 mg and 1 mg concentration of the catalyst was taken in 5 mL of dye (0.2mM). This reaction was performed under sunlight irradiation

and in dark for 30 min. Change in the UV-Visible spectra was observed after 30 min as seen in figure 18.

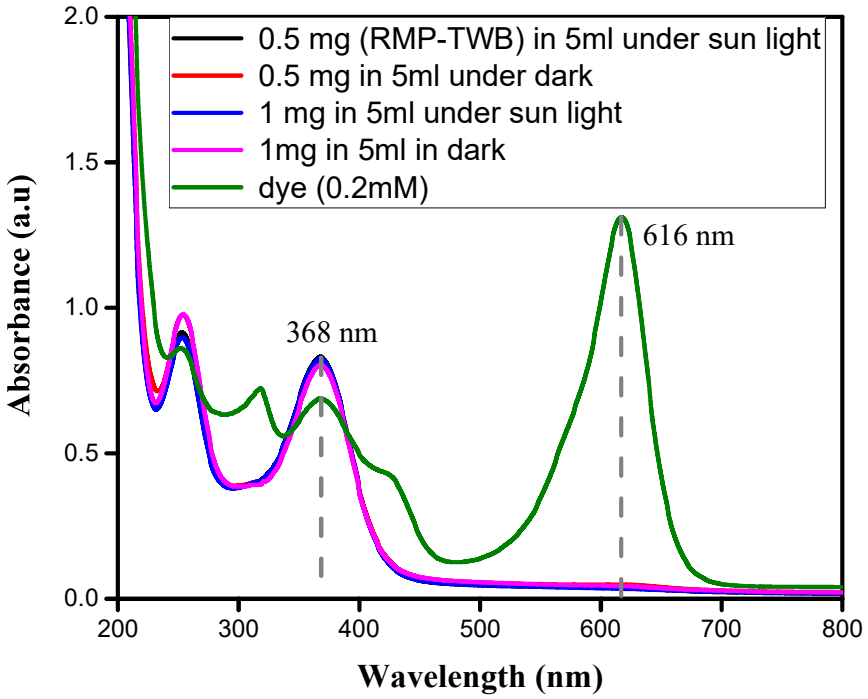

Fig.18: Changes in UV absorption spectra of MG dye (0.2 mM in 5ml) due to its photo degradation by different amount of RMP-TWB (900°C) sample under 30 min sun light irradiation.

0.5 mg and 1 mg concentration of RMP-TWB was taken in 15 mL of dye (0.2mM). This reaction was performed under dark as well as sunlight irradiation at different time intervals. Change in the UV-Visible spectra was observed after regular intervals of time as seen in figure 19.

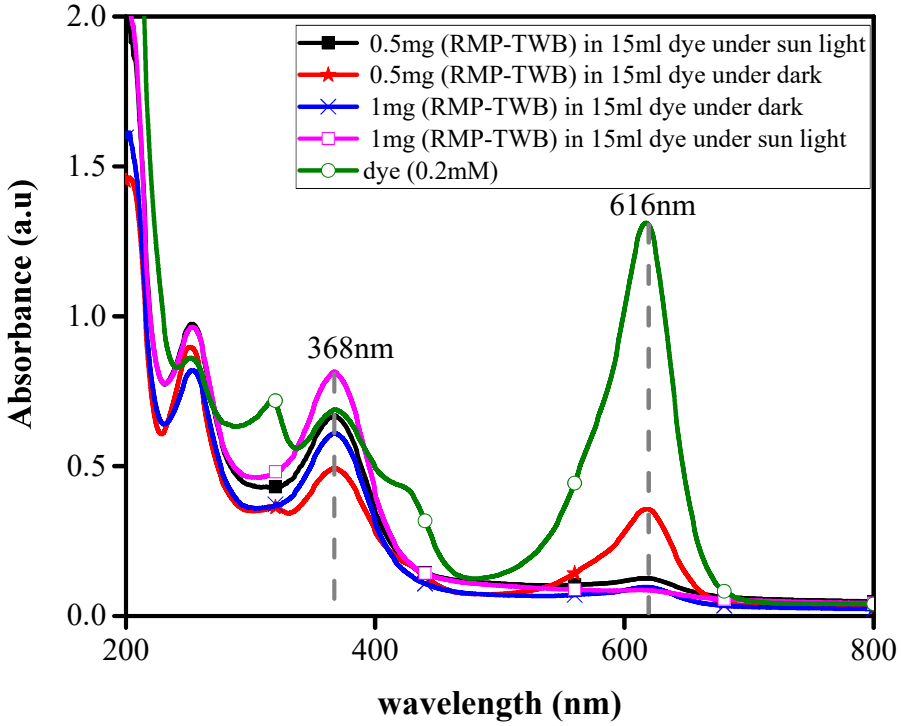

Fig.19: Changes in UV absorption spectra of MG dye (0.2 mM in 15 ml) due to its photo degradation by different amount of RMP-TWB (900°C) sample under 30 min sun light irradiation and their color changes.

0.5 mg of RMP-TWB was taken in 30 mL of dye (0.2mM). This reaction was performed under sunlight irradiation at different time intervals. Change in the UV-Visible spectra was observed after regular intervals of time. The results show that after 60 min of the reaction maximum degradation of MG was observed from figure 20 (a).

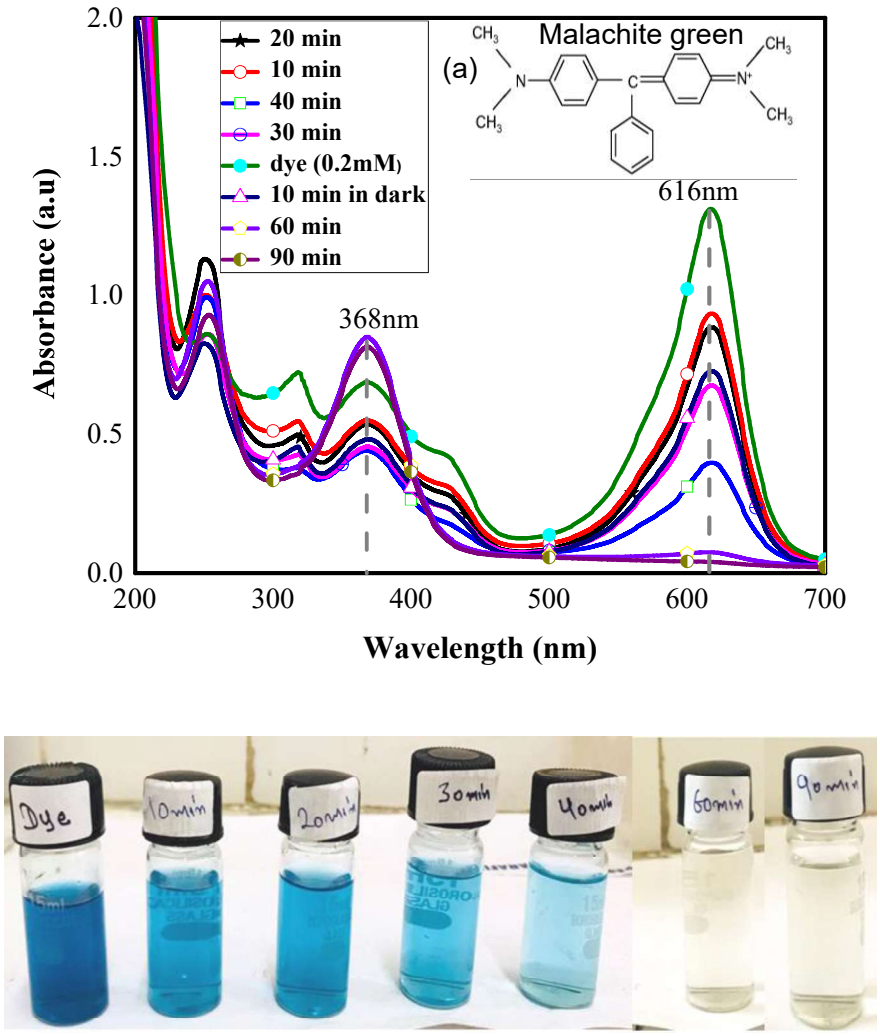

Fig.20: (a) Changes in UV absorption spectra of MG dye (0.2 mM in 30 ml) due to its photo degradation by 0.5 mg amount of RMP-TWB (900ºC) under sun light irradiation and their color changes.

The kinetic study of the degradation of MG has been shown in figure 20 (b) w.r.t. zero and first order reaction. The equation for zero order and first order reaction as given below

$$[A]_0 - [A]_t = kt \qquad \ln C_0 / C_t = kt$$

Where C_t and $[A]_t$ the concentration of the reactant after the degradation (mol/l), C_0 and $[A]_0$ the concentration of reactant before degradation, t the irradiation time (min). k is rate constant of the pseudo-first-order (min^{-1}) reaction. It was concluded that fitting of first-order reaction was better than zero order reaction which is shown by the value of R2 (regression coefficient).

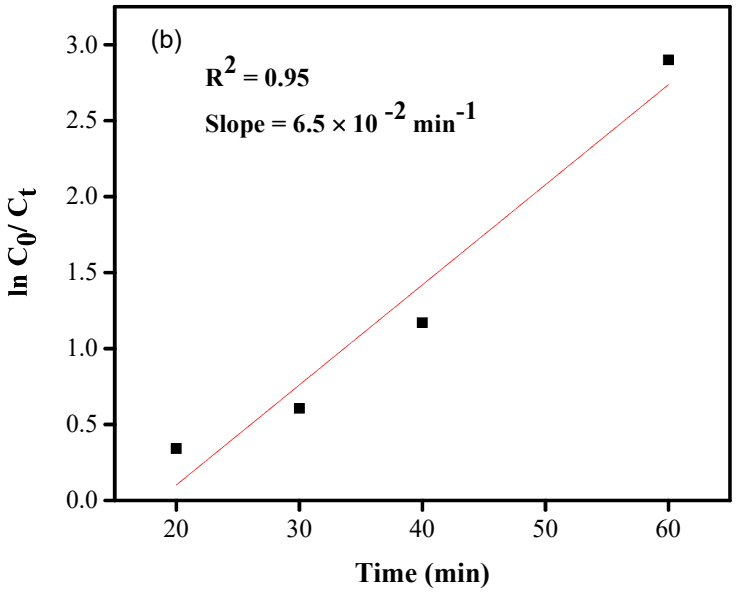

The value of R^2 (0.98 and 0.95) and slope (31×10^{-4} Ms^{-1} and 6.5×10^{-2} min^{-1}) for the zero and first order respectively.

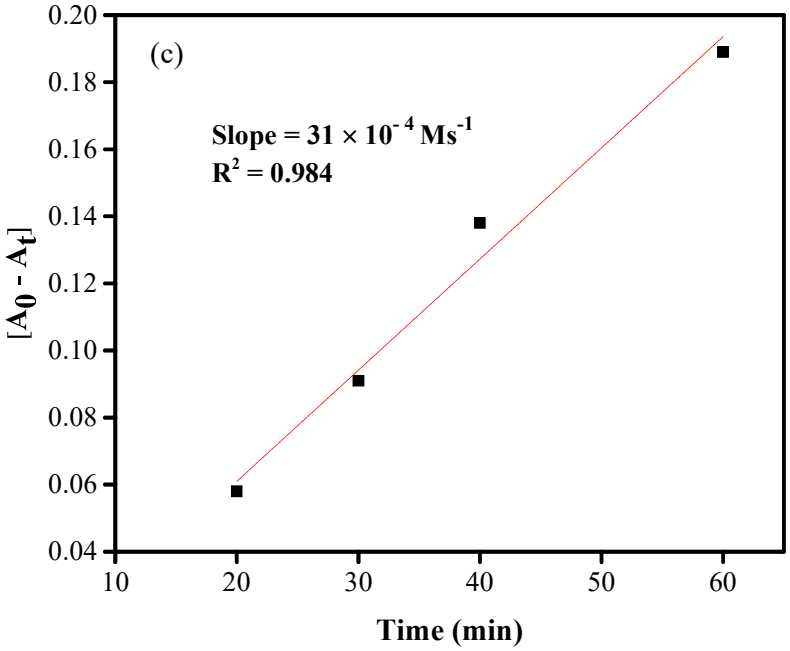

Fig.20: Kinetic studies showing the rate constant (b) first order (c) zero order obtained for photocatalytic degradation of MG dye under sunlight.

Similarly, 1 mg concentration of RMP-TWB was taken in 30 mL of dye (0.2mM). This reaction was performed under sunlight irradiation at different time intervals. Change in the UV-Visible spectra was observed after regular intervals of time. The results show that after 60 min of the reaction maximum degradation of MG was observed from figure 21 (a).

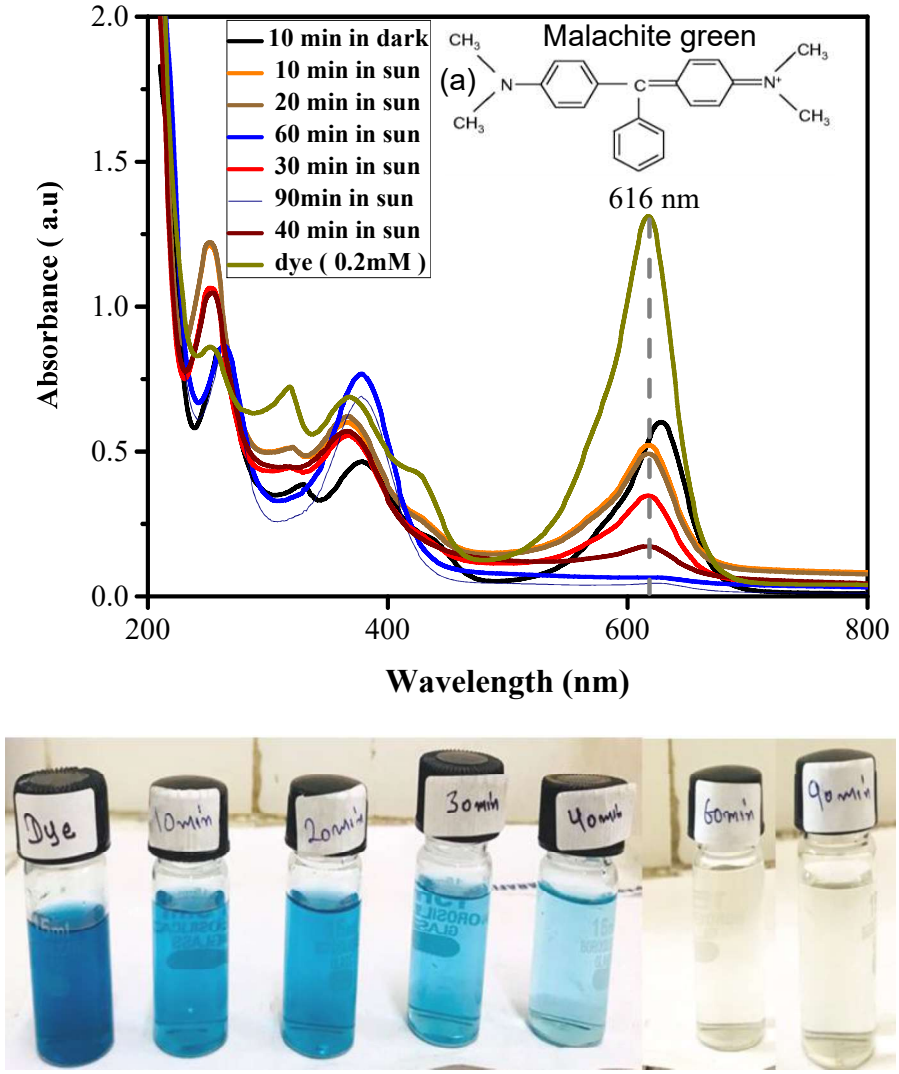

Fig.21: (a) Changes in UV absorption spectra of MG dye (0.2 mM in 30 ml) due to its photo degradation by 1 mg amount of RMP-TWB (900°C) under sun light irradiation and their color changes.

The kinetic study of the degradation of MG has been shown in Figure b w.r.t to zero and first order reaction. The equation for zero order and first order reaction

$[A]_0 - [A]_t = kt$ $\ln C_0 / C_t = kt$

C_t and $[A]_t$ the concentration of the reactant after the adsorption step (mol/l), C_0 and $[A]_0$ the concentration of reactant before adsorption, t the irradiation time (min). k is rate constant of the pseudo-first-order (min^{-1}) reaction. We concluded that fitting of first-order reaction was better than zero order reaction which is shown by the value of R2 (regression coefficient). The value of R^2 (0.92 and 0.99) and slope (17×10^{-4} Ms^{-1} and 5.6×10^{-2} min^{-1}) for the zero and first order respectively.

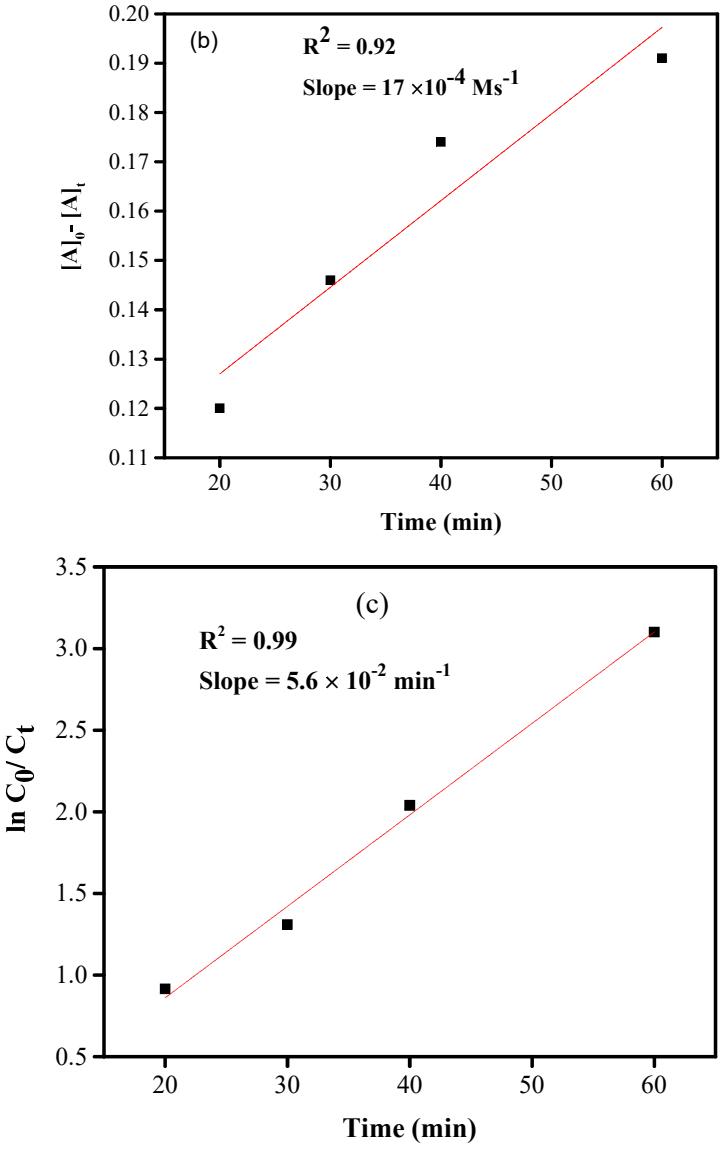

Fig.21: Kinetic studies showing the rate constant (b) zero order (c) first order obtained for photocatalytic degradation of MG dye under sunlight.

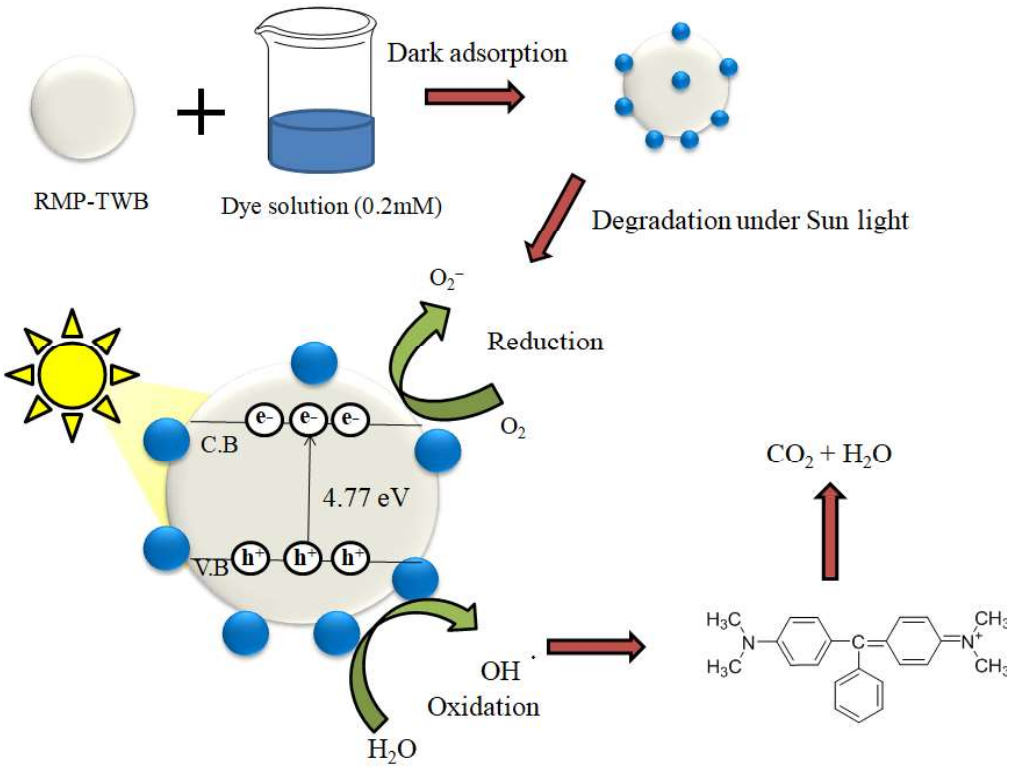

Scheme 2: Mechanism of adsorption and degradation of MG over RMP-TWB.

Conclusion

The method of extraction of RMP-TWB was cost-effective, nontoxic and eco-friendly. The obtained residue was used for the adsorption and immediate degradation of MG dye. It was characterized by using DLS, XRD, SEM, FTIR, BET and UV- Visible spectroscopy with various techniques. The surface area and mean pore diameter of RMP-TWB was 35.4m^2g^{-1}and10.08 nm respectively. XRD data revealed that RMP-TWB contains the majority of the calcium carbonate and some amount of MgO, SiO_2.The obtained residue was calcinated at 900^oC resulting in the decomposition of $CaCO_3$ to CaO which can be further used for the synthesis of bio-diesel. In future, the residue obtained (RMP-TWB) from tap water further used in the formation of chalk, in paints, and adsorption and complete removal of various industrial dyes.

References

1. Ong, C.; Ibrahim, S.; Sen Gupta, B., A survey of tap water quality in Kuala Lumpur. *Urban Water Journal* **2007,** *4* (1), 29-41.

2. Zhu, Y.; Narukawa, T.; Inagaki, K.; Miyashita, S.-i.; Kuroiwa, T.; Ariga, T.; Kudo, I.; Koguchi, M.; Heo, S. W.; Suh, J. K., Development of a Certified Reference Material (NMIJ CRM 7203-a) for Elemental Analysis of Tap Water. *Analytical Sciences* **2017,** *33* (3), 403-407.

3. Kadam, T.; Kulkarni, M., EFFECT OF WATER HARDNESS ON FOAMING BEHAVIOUR IN JET DYEING. *BTRA Scan* **2016,** *46* (3).

4. Singh, V. K.; Ramprakash, R.; Kumar, S., Evaluation of Groundwater Quality for Irrigation in Gulha Block of Kaithal District in Haryana. *Journal of Soil Salinity and Water Quality* **2017,** *9* (2), 241-248.

5. Bharadwaj, N. D.; Mishra, P.; Sharma, A.; Uchchariya, D., Reduction of Total Hardness of Water Using Phyllanthus emblica. *Imperial Journal of Interdisciplinary Research* **2016,** *2* (7).

6. Boyd, C. E., Total Hardness. In *Water Quality*, Springer: 2015; pp 179-187.

7. Itsadanont, S.; Theptat, P.; Scamehorn, J. F.; Soontravanich, S.; Sabatini, D. A.; Chavadej, S., Dissolution of soap scum by surfactants. Part III. Effect of chelant type on equilibrium solubility and dissolution rate of calcium and magnesium soap scums in various surfactant systems. *Journal of Surfactants and Detergents* **2015,** *18* (6), 925-932.

8. Barhoum, A.; Rahier, H.; Abou-Zaied, R. E.; Rehan, M.; Dufour, T.; Hill, G.; Dufresne, A., Effect of cationic and anionic surfactants on the application of calcium carbonate nanoparticles in paper coating. *ACS applied materials & interfaces* **2014,** *6* (4), 2734-2744.

9. Boyjoo, Y.; Pareek, V. K.; Liu, J., Synthesis of micro and nano-sized calcium carbonate particles and their applications. *Journal of Materials Chemistry A* **2014,** *2* (35), 14270-14288.

10. Ameta, R.; Kumar, D.; Jhalora, P., Photocatalytic degradation of methylene blue using calcium oxide. *Acta chim Pharma Indica* **2014,** *4* (1), 20-28.

11. Zhao, M.; Chen, Z.; Lv, X.; Zhou, K.; Zhang, J.; Tian, X.; Ren, X.; Mei, X., Preparation of core–shell structured CaCO3 microspheres as rapid and recyclable adsorbent for anionic dyes. *Royal Society open science* **2017,** *4* (9), 170697.

12. Zhang, H.-b.; Chen, N.-h.; Tong, Z.-f.; Liu, Q.-f.; Tang, Y.-k.; Zhou, Z.-l.; Shi, H.-z., Adsorption of Methylene Blue and Congo Red on Bentonite Modified with CaCO 3. *Key Engineering Materials* **2017,** *727*.

13. Mansir, N.; Hin, T.-Y. Y., Synthesis and characterization of solid heterogeneous catalyst for the production of biodiesel from high FFA waste cooking oil. *Bayero Journal of Pure and Applied Sciences* **2017,** *10* (1), 62-66.

14. Madhusudhana, N.; Yogendra, K.; Mahadevan, K., A comparative study on Photocatalytic degradation of Violet GL2B azo dye using CaO and TiO2 nanoparticles. *Int J Eng Res Appl* **2012,** *2* (5), 1300-1307.

15. Banković–Ilić, I. B.; Miladinović, M. R.; Stamenković, O. S.; Veljković, V. B., Application of nano CaO–based catalysts in biodiesel synthesis. *Renewable and Sustainable Energy Reviews* **2017,** *72*, 746-760.

16. Yagub, M. T.; Sen, T. K.; Afroze, S.; Ang, H. M., Dye and its removal from aqueous solution by adsorption: a review. *Advances in colloid and interface science* **2014,** *209*, 172-184.

17. Khamparia, S.; Jaspal, D.; Malviya, A., Optimization of adsorption process for removal of sulphonated di azo textile dye. *Green Chemistry & Technology Letters* **2015,** *1* (01), 61-66.

18. Asiltürk, M.; Sayılkan, F.; Arpaç, E., Effect of Fe3+ ion doping to TiO2 on the photocatalytic degradation of Malachite Green dye under UV and vis-irradiation. *Journal of Photochemistry and Photobiology A: Chemistry* **2009,** *203* (1), 64-71.

19. Georgiadis, I.; Papadopoulos, A.; Kantiranis, N.; Filippidis, A.; Tsirambides, A., sorption of MalaChite green froM aqueous solutions onto greek raW diasporiC bauxite. *Journal of Environmental Protection and Ecology* **2014,** *15* (2), 606-615.

20. Rodriguez-Blanco, J. D.; Shaw, S.; Benning, L. G., The kinetics and mechanisms of amorphous calcium carbonate (ACC) crystallization to calcite, via vaterite. *Nanoscale* **2011,** *3* (1), 265-271.

21. Ogino, T.; Suzuki, T.; Sawada, K., The formation and transformation mechanism of calcium carbonate in water. *Geochimica et Cosmochimica Acta* **1987,** *51* (10), 2757-2767.

22. Galvan-Ruiz, M.; Baños, L.; Rodriguez-Garcia, M. E., Lime characterization as a food additive. *Sensing and Instrumentation for Food Quality and Safety* **2007,** *1* (4), 169-175.

23. Tan, Y. H.; Davis, J. A.; Fujikawa, K.; Ganesh, N. V.; Demchenko, A. V.; Stine, K. J., Surface area and pore size characteristics of nanoporous gold subjected to thermal, mechanical, or surface modification studied using gas adsorption isotherms, cyclic voltammetry, thermogravimetric analysis, and scanning electron microscopy. *Journal of materials chemistry* **2012,** *22* (14), 6733-6745.

24. Liu, Y.; Jiang, Y.; Hu, M.; Li, S.; Zhai, Q., Removal of triphenylmethane dyes by calcium carbonate–lentinan hierarchical mesoporous hybrid materials. *Chemical Engineering Journal* **2015,** *273*, 371-380.

25. Madhusudhana, N.; Yogendra, K.; Mahadevan, K. M., Photocatalytic degradation of violet GL2B azo dye by using calcium aluminate nanoparticle in presence of solar light. *Research Journal of Chemical Sciences* **2012,** *2231*.